Comparison Study of Dynamic Models For Satellite Formation Flying

Hang Yue

School of Electrical & Electronic Engineering

A thesis submitted to the Nanyang Technological University

in fulfillment of the requirements for the degree of

Master of Engineering

2008

Statement of Originality

I hereby certify that the content of this thesis is the result of work done by me and has not been submitted for a higher degree to any other University or Institution.

July 31st 2008
Date

Hang Yue
Hang Yue

Acknowledgments

I would like to thank my supervisor, Professor Wang Dan Wei, for his continuous support, patience, guidance, advice and encouragement forwards the completion of my master program. He is a very nice mentor. His insightful comments and suggestions always inspire me for my research work. I would also like to thank my co-supervisor, Associate Professor Poh Eng Kee, in every meeting with DSO colleagues, his comments always provide guidance and direction for me. He greatly facilitate our group research work.

Also I would like to thank our group members, Dr. Xu Guangyan, Mr. Wu Baolin, for their great assistance during two years of my postgraduate study at Nanyang Technological University. Without their help, I would have never completed this milestone. I am grateful to all my colleagues in Intelligent Robotics Lab and Aerospace Electronics Lab. They are very friendly and helpful.

Lastly, and most importantly, I would like to thank my family for their moral support and sacrifice. In particular, I want to thank my wife Zhou Li, for her constant love, care and understanding. Without them, I would have never completed this thesis.

Summary

This thesis focuses on the comparison of dynamic models for satellite formation flying with the aid of simulation platforms Satellite Tool Kit (STK) and Matlab.

One key challenge in formation flying technology is to model satellite relative dynamics. Based on the relative motion dynamic models, we can develop formation design and control strategies. Much work has been done concerning the relative motion of two satellites. In this thesis, firstly, a review is conducted on dynamic models of satellite formation flying. Then STK and Matlab will be used to evaluate the impact of different orbital perturbations on several linearized model. Later a model error index will be introduced to compare the accuracy of various dynamic models. Finally, the simulation results and analysis are presented.

The main contributions of this thesis include:

- Model error and perturbation effects: orbital perturbation effects on various dynamic models are studied and evaluated in simulation platforms.
- Dynamic model accuracy: Based on a newly defined model error index and simulation method, the accuracies of six typical dynamic models are analyzed. The simulation results can provide space mission designer useful information on dynamic model selection.

Table of Contents

Acknowledgments i

Summary ii

List of Figures vi

List of Tables viii

1 Introduction 1

1.1 Background 1

1.2 Motivation and Approach 4

1.3 Major Contributions of the Thesis 5

1.4 Outline of the Thesis 5

2 Fundamentals 7

2.1 Coordinate Systems 7

2.1.1 Earth Centered Inertial Coordinate 7

2.1.2 Orbital Elements 8

2.1.3 LVLH Coordinate 9

2.2 Orbital Perturbations 9

3 Review of Dynamic Models 13

3.1 Background 13

3.2 Dynamic Models 15

3.2.1 Hill's Equations (HCW model) 15

3.2.2 TH Model 19

3.2.3 Schweighart and Sedwick Model 21

3.2.4 Tillerson and How Model 23

3.2.5 Unperturbed Nonlinear Model 24

3.2.6 Xu-Wang Model 25

4 Comparison Study of Models 28

4.1 Objective 28

4.2 Model Comparison Method 29

4.3 Simulation Platform 30

4.4 Simulation in STK 32

4.4.1 Creation of a Scenario 32

4.4.2 Selection of Propagator 34

4.4.3 Data Processing 36

4.5 Interface of STK and Matlab 36

4.6 Model Error Index 38

5 Model Error Study: Perturbation Effects 40

5.1 Simulation Scenario 40

5.2 Simulation Results and Discussion 41

5.2.1 Orbit Eccentricity 41

5.2.2 J_2 Disturbance 44

5.2.3 Atmospheric Drag and Solar Radiation 46

6 Model Error Study: Comparison **48**

6.1 Simulation Scenario 48

6.2 Simulation Results 51

6.2.1 Error Index vs Formation Size ρ 51

6.2.2 Error Index vs Chief Orbit Eccentricity e 54

6.2.3 Error Index vs Chief Orbit Inclination i 59

6.2.4 Error Index Vs Semi-major Axis a 64

7 Conclusions and Future Works **66**

7.1 Conclusions 66

7.1.1 Insights of Simulation Comparison 66

7.1.2 Comparison of Direct ODE models 69

7.2 Future Works 69

Bibliography **71**

List of Figures

2.1 Earth Centered Inertial Coordinate System 8

2.2 LVLH coordinate system 9

2.3 Origin of Earth oblateness perturbation 10

4.1 Function Chart of Model Comparison Method 29

4.2 STK Astrogator Orbit Initial State 33

4.3 Set Deputy Satellite Reference Vehicle 34

4.4 Satellite Parameters Configuration 34

4.5 STK Astrogator Propagator Configuration 35

4.6 Relative Motion between Chief and Deputy Satellite Plotted by STK 36

5.1 HCW Model Error with Small Chief Orbit Eccentricity 0.005 42

5.2 TH Model Error with Chief Orbit Eccentricity 0.005 43

5.3 HCW Model Error under J_2 Perturbation 44

5.4 TH Model Error under J_2 Perturbation 45

5.5 Schweighart and Sedwick Model Error under J_2 Perturbation 46

5.6 HCW Model Error under Atmospheric Drag and Solar Radiation Effect 47

6.1 Index Comparison for $e = 0.0001$, $i = 45°$, $a = 6600km$ 51

6.2 Index Comparison for $e = 0.0001$, $i = 45°$, $a = 8000km$ 52

6.3 Index Comparison for $e = 0.01$, $i = 45°$, $a = 6600km$ 53

6.4 Index Comparison for $e = 0.01$, $i = 45°$, $a = 8000km$ 54

6.5 Index Comparison for $\rho = 0.1km$, $i = 45°$, $a = 6600km$ 55

6.6 Index Comparison for $\rho = 0.1km$, $i = 45°$, $a = 8000km$ 57

6.7 Index Comparison for $\rho = 20km$, $i = 45°$, $a = 6600km$ 58

6.8 Index Comparison for $\rho = 20km$, $i = 45°$, $a = 8000km$ 59

6.9 Index Comparison for $\rho = 0.1km$, $e = 0.0001$, $a = 8000km$ 60

6.10 Index Comparison for $\rho = 0.1km$, $e = 0.01$, $a = 8000km$ 61

6.11 Index Comparison for $\rho = 20km$, $e = 0.0001$, $a = 8000km$ 62

6.12 Index Comparison for $\rho = 0.1km$, $e = 0.0001$, $a = 6600km$ 63

6.13 Index Comparison for $\rho = 0.1km$, $e = 0.0001$, $i = 45°$ 64

6.14 Index Comparison for $\rho = 0.1km$, $e = 0.01$, $i = 45°$ 65

List of Tables

4.1 Orbital elements of chief satellite 32

4.2 Relative Position of Deputy Satellites 33

5.1 Comparison study formulation 40

5.2 Orbital parameters of chief satellite 41

6.1 Orbital Elements of Chief Satellite 49

6.2 Parameters of Deputy Satellite and Formation 49

6.3 Satellite Parameters Configuration 49

7.1 Comparison of direct ODE models 69

Chapter 1

Introduction

1.1 Background

Autonomous formation flying of multiple small satellites to replace a single large satellite will be an enabling technology for a number of future space missions. Potential applications include synthetic apertures for surveillance and interferometry missions, or for field measurements and atmospheric survey missions. Though there are potential limitations, the benefits of using multiple spacecrafts are obvious. It can increase the reliability and redundancy of the whole system, reduce the cost of launching and maintenance, greatly widen the surveillance area and add more flexibility into the mission design. For instance, a ground observing sensor can be carried by several satellites flying in a specified formation to increase aperture size rather than construct a large and much more expensive single satellite. With a single satellite, the whole mission will be aborted in the event of satellite failure. However, a failed satellite in a formation can be mitigated in the sense that mission can be re-organized using remaining member satellites in the formation. In addition, formation flying technology enables us to easily add more satellites into the mission or upgrade any satellites. There are a number of missions which ben-

efit from satellite formation in either Low Earth Orbit (LEO) or deep space. For example, TechSat21[19] and Orion/Emerald[14], though never launched, paved the way for cooperative satellite operations. Several missions have been deployed, including EO-1/LandSat7[6], GRACE[33], CLUSTER II/Phoenix[10], ST5[18], and FORMOSAT-3/COSMIC[39]. In addition, several missions are in the planning stage, such as Magnetospheric Multiscale Mission (MMS)[9] and ST9[21]. All of the missions have prescribed relative motion and attitude requirements, which are designed to meet specific objectives.

With the desire to insert satellites in a formation comes the need to predict accurate relative position and velocity between the satellites. In other words, to describe the relative motion of satellites in a formation is the first and most important problem that needs to be addressed. To study the relative motion, much effort has been made in this area. Researchers initially use a set of linearized differential equations, i.e.,Hill's equations[13], which is also known as Clohessy-Wiltshire equations[8], to describe the relative motion of two satellites in near-circular orbits. This was a logical first step since Hill's equations are simple and easy to implement. In addition, it had been successfully used to predict the relative motion between two satellites in rendezvous scenario. However, rendezvous scenario usually takes a short time, thus the model error is insignificant and may be ignored. In contrast, satellite formation flying occurs over a much longer period, and the model error will accumulate over time and the solution becomes erroneous. Also, there are some inherent limitations of Hill's equations, such as near-circular orbit assumption, no disturbances considered and so on, which make its accuracy unacceptable in practical application.

To develop a simple, linearized and more accurate dynamic model for formation design, guidance and control, researchers have actively worked on this problem. Sabol.et.al[26] investigated several formation flying designs using Hill's equations. Yeh and Sparks[41] studied the geometrical insight of Hill's equations and obtain parametric equations describing desired formation. Schaub and Alfriend[29] pre-

sented an analytical method to establish J_2 invariant relative orbits, though their resultant orbit radial is too large for practical implementatoin. In a later work by Vadali et al.[37], a linearized combination of Hill's equations with the J_2 effect was developed. The resulting equations are linear with periodic coefficients, and differencing them produces a homogeneous set of equations that can be numerically integrated to track the relative motion of two satellites with the same accuracy as their nonlinear simulation for periods up to one day.

Generally speaking, we can classify these dynamic models into three categories. The first category is the direct ODE (Ordinary Differential Equations) models, which described the relative motion in local reference satellite fixed frame. This category of models mostly are extensions or modifications of Hill's equations[35][30] [34][40]. Because these models are in the form of differential equations, they have significant applications in controller design.

The second category is indirect models, which are usually expressed in differences of orbital elements[29][27][28][7][17]. Because satellite orbit can be easily represented by orbital elements, it is easier to use orbital elements differences to design satellite formation. Also, using orbital elements differences avoids rounding error, which is introduced in coordinate transformation.

The third category is the solution-based models, which are usually in the form of STM (State Transition Matrix)[11][32][23][20]. Using STM, we can directly generate accurate satellite motion though it is very complicated. Duc to STM complexity, they are more applicable in propagation simulation rather than formation design and control.

1.2 Motivation and Approach

Over the past few years there has been a growing interest in satellite formation flying, and much research has been done to explore the use of satellite formation flight for such missions as a space-based radar or interferometry. In these missions, a "virtual" satellite comprising of several micro/mini satellites in a formation has significant cost reduction and performance advantage over single large satellite for applications such as distributed aperture remote sensing, geo-location and superior angular resolution. Such formations are investigated by the US Air Force Research Lab, NASA and other European astronautic research organizations.

In order to manage and control multiple satellites as a virtual satellite, the first step is to derive an accurate dynamic model of a satellite cluster, which can predict relative motion between the satellites. Our current work focuses on inter-satellite positioning dynamic model evaluation and development. From the literature review, we know that the complexity of the relative motion dynamic models increases as the required accuracy is greater. The available models were developed under different assumptions and by different methodologies. A comparison study will help to understand the pros and cons of each case. By comparison study, we can find a way to select an appropriate model for a specific mission and determine what kind of perturbation should be considered for specific applications.

In this thesis, the comparison approach is by scenario definition and simulation study. We propose a simulation-based method and a model error index. Commercial satellite software STK[3] (Satellite Tool Kit) is used as benchmarking tool to compare various dynamic models. Also, the simulation results will be analyzed for future dynamic model development and satellite formation flight mission design.

1.3 Major Contributions of the Thesis

This work aims to study, evaluate and compare various dynamic models for satellite formation flying under different orbital circumstances. The major contributions include:

- Model error and perturbation effects: different orbital perturbations on various dynamic models are studied and evaluated in simulation platform.
- Dynamic model accuracy comparison:
  - A simulation-based framework is presented to compare various dynamic models
  - A model error index is proposed and used in simulation evaluation of various dynamic models
  - Simulation results provide a space mission designer valueable information on dynamic models and orbital perturbation.

1.4 Outline of the Thesis

The outline of the thesis is as follows:

- Chapter 2 explains fundamentals of orbital mechanics which form the basis of satellite formation flying and introduces:
  - Special coordinate systems of formation flying including Earth Centered Inertial (ECI) Coordinate, Local Vertical Local Horizontal (LVLH) Coordinate and Orbital Elements.
  - Orbital perturbations such as Earth oblateness Effects (J_2) and atmospheric drag

- Chapter 3 reviews dynamic models for satellite formation flying and includes:
  - background of dynamic models development
  - Review of dynamic models in literature.
- Chapter 4 introduces comparison method and simulation platform. It contains:
  - Objective of comparison study
  - Model comparison framework.
  - A brief introduction to STK. The reason of its adoption for our research.
  - A brief demonstration of running simulation in STK including interface coding and simulation environment.
  - Introduction to the model error index
- Chapter 5 studies model error under different perturbations and comprises two parts:
  (1) Simulation scenarios and parameter definitions
  (2) Simulation results and discussions
- Chapter 6 compares different dynamic model accuracy using model error index and contains:
  (1) Simulation scenarios and parameter definitions
  (2) Simulation results, discussions and comparisons
- Chapter 7 provides conclusions and recommends future works. It summarizes:
  - Insights derived from simulation comparison study
  - Comparison of direct ODE models
  - Future works

Chapter 2

Fundamentals

2.1 Coordinate Systems

As the basis for study and development, the coordinate systems used throughout the thesis are described in this chapter. One coordinate frame is Earth Inertial system, and is used to represent absolute position of whole satellite formation. The second coordinate frame is body fixed coordinate system, and is used to represent the relative motion of individual satellites.

2.1.1 Earth Centered Inertial Coordinate

The Earth Inertial coordinate system has its origin at the Earth centre and is also called $\hat{X}$-$\hat{Y}$-$\hat{Z}$ inertial coordinate system. Its origin lies at the Earth's center. The fundamental plane is the equator, and the positive $\hat{X}$ axis points in the vernal equinox direction. The $\hat{Z}$ axis points in the direction of the North Pole. $\hat{Y}$ axis completes the right-hand orthogonal triad. The geocentric-equatorial coordinate system is shown in Figure 2.1. We use this coordinate system to describe the absolute motion of a satellite in space.

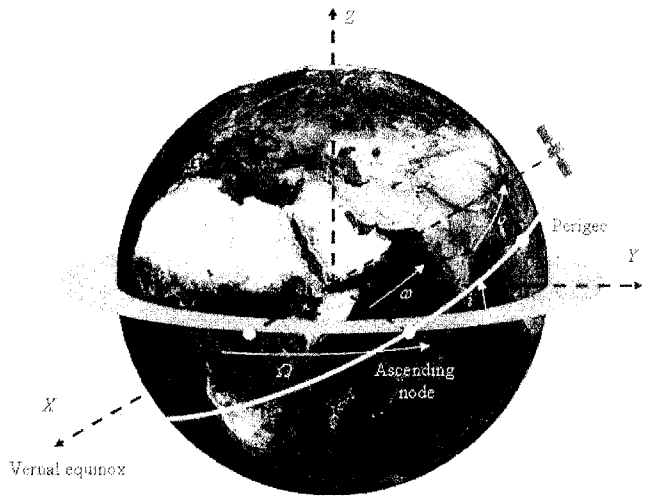

Figure 2.1: Earth Centered Inertial Coordinate System

2.1.2 Orbital Elements

The motion of a satellite around Earth may be described mathematically by three scalar second-order differential equations. The integration of these equations of motion yields six elements of integration. These elements of integration are known as the orbital elements. Also see Figure 2.1, they are

- a is semi-major axis, which specifies the size of a orbit
- e is eccentricity, which specifies the shape of the orbit
- v is true anomaly, which determines the satellite's current position relative to the location of periapsis.
- i is inclination of the orbit plane with respect to the reference plane (Earth's equator plane).
- Ω is right ascension of the ascending node.
- ω is argument of perigee.

2.1.3 LVLH Coordinate

The second coordinate system is a body fixed coordinate system, which is known as local vertical local horizontal (LVLH) frame with the origin located at the reference satellite. We use this frame for the relative motion between satellites in a formation. As shown in Figure 2.2, the $\hat{x}$ axis is defined as pointing from the Earth's center along the radius vector toward the satellite as it moves along the orbit, and $\hat{z}$ axis is fixed along the direction of orbital angular momentum vector. The $\hat{y}$ axis completes the right hand system. When we are describing relative position or displacements in LVLH frame, notations of "Radial", "Along-track" and "Cross-track" are usually used to denote directions of $\hat{x}$, $\hat{y}$, $\hat{z}$, respectively.

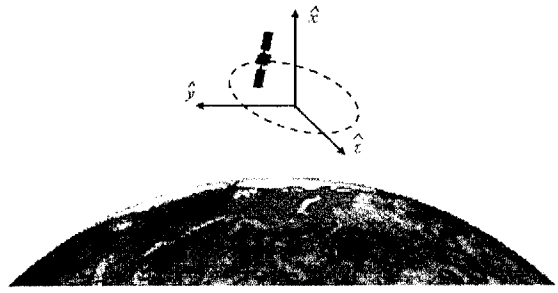

Figure 2.2: LVLH coordinate system

2.2 Orbital Perturbations

Perturbations are deviations from a normal, idealized, or undisturbed motion. The actual motion will vary from an ideal undisturbed path (two-body) due to perturbations caused by other bodies (such as Sun and Moon) and additional forces not considered in Keplerian motion (such as non-spherical Earth and atmospheric drag).

(1) Earth Aspherical Perturbation

The aspherical nature of Earth, arising from the equatorial bulge (equatorial

radius-polar radius=21km, shown in Figure 2.3) leads to a gravitational attraction on a body that is no longer directed towards the center of mass of the Earth. From Newton's law of gravitation, the gravitational acceleration vector, $d\vec{a}$, due to the infinitesimal mass dm of the body of arbitrary shape in Figure 2.3 is given by

$$d\vec{a} = -Gdm\frac{\vec{\rho}}{\rho^3} \tag{2.1}$$

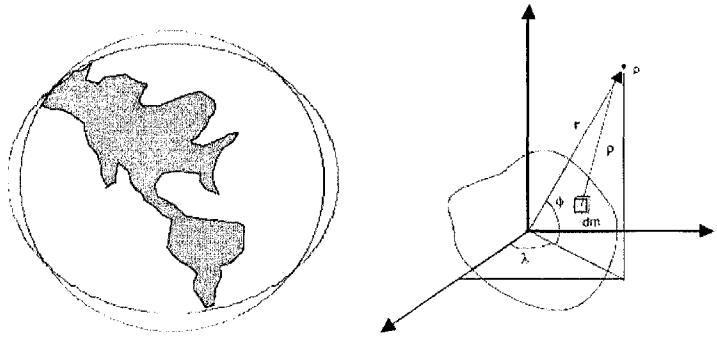

Figure 2.3: Origin of Earth oblateness perturbation

where $G = 6.672 \times 10^{-11} kg^{-1}m^3s^{-2}$ is the universal gravitational constant, $\vec{\rho}$ is a vector pointing from the infinitesimal mass to point P in Figure 2.3. If Φ is a potential function, the acceleration in the field is given by

$$\frac{d^2\vec{r}}{dt^2} = -\nabla\Phi = -\left[\frac{\partial\Phi}{\partial x}i_x + \frac{\partial\Phi}{\partial y}i_y + \frac{\partial\Phi}{\partial z}i_z\right] \tag{2.2}$$

where i_x,i_y,i_z denote unit vectors in the frame of Figure 2.3. The potential due to an elemental mass, dm, is therefore given by

$$d\Phi = -\frac{Gdm}{\rho} \tag{2.3}$$

In spherical coordinates, the point P in Figure 2.3 has the coordinates (r, ϕ, λ) where r is the radial distance, ϕ, is the geocentric latitude, and λ is the longitude. For a body with rotational symmetry, the gravitational potential

is independent of λ and can be obtained by integrating Eq.2.3 over the entire volume of the body, to obtain

$$\Phi(r,\phi) = \frac{\mu}{r}\left[1 + \sum_{k=2}^{\infty} J_k \left(\frac{R_e}{r}\right)^k P_k(\sin\phi)\right] \tag{2.4}$$

where $\mu = GM_e$(M_e is the mass of the Earth), R_e is Earth radius, J_k represent the constant coefficients and P_k is the kth Legendre polynomial. Since the mass distribution is the same with respect to the axis of rotation, the potential does not depend on the longitude. Our research focuses on the effects of the second zonal harmonic J_2 since it is the most dominant among the harmonics. The second zonal harmonic for the Earth has the following value:

$$J_2 = 1.082629 \times 10^{-3} \tag{2.5}$$

The other harmonics are of the order of 10^{-6} or less.

(2) Atmospheric Drag

Atmospheric forces represent the largest non-gravitational perturbations acting on low altitude satellites. The dominant atmospheric force, called drag, directly opposes the velocity of the satellite motion and is a function of the surface area of individual satellite. Hence, a faster and larger satellite will experience more atmospheric drag.

(3) Solar-radiation Pressure

A satellite that is exposed to solar radiation experiences a small force that arises from the absorption or reflection of photons. In contrast to gravitational perturbations, the acceleration due to the solar radiation depends on the satellite's mass and surface area.

(4) Other Perturbations such as third-body attraction and so on.

For low Earth orbit formation flying missions, the last two perturbations are much smaller than Earth aspherical perturbation and atmospheric drag. Thus, most

researchers focus on modeling the effect of J_2 disturbance and developing control forces to compensate the other perturbations.

Chapter 3

Review of Dynamic Models

3.1 Background

The study of relative dynamics of two satellites begins in the early 1960s, when Clohessy and Wiltshire[8] published their paper about satellite rendezvous technology, which is popularly known as the CW or Hill's equations (HCW model). Hill's equations[13] are established based on the assumptions that the chief satellite orbit is a circle and the Earth gravitational field is spherically symmetrically distributed. Since the spacecraft rendezvous scenario in their paper occurs in a small eccentric orbit in a short duration, Hill's equations' solutions are appropriate. Hill's equations yield simple analytical solutions, which offered a number of benefits to the formation design and analysis to achieve optimal controller design with strict fuel consumption constraints. However, when researchers investigated satellite formation flight with much longer duration time and included various orbital disturbances. The accuracy of Hill's equations is far from adequate. Dynamic model error results in higher control efforts and more fuel consumption for long duration formation flying.

The model error of Hill's equations comes from three aspects: nonlinearity of

dynamics, eccentricity of chief satellite orbit, and perturbations. In low Earth orbit environment, the Earth oblateness perturbation (J_2) is the dominant effect. Therefore, high fidelity dynamic model must incorporate eccentricity, nonlinearity and J_2 perturbation. This model would lay a foundation for the study of satellite formation dynamics, design, guidance and control.

Following Hill's equations, the direct ODE models(see Section 1.1) evolved in these steps: Hill's equations were first extended to unperturbed relative motion that take into account eccentricity or/and nonlinearity. Tschauner and Hempel[35] first solved the satellite relative motion in elliptical orbits. Their linearized model is called TH equations or TH model. Analytical solution of TH model can be both obtained in true anomaly domain and time domain. Inalhan and How[15] proposed initial conditions of TH model to obtain a periodic motion. Then Hill's equations were extended to include J_2 perturbations in circular orbit. Ross[25] firstly introduced J_2 components to Hill's equations and obtained a set of LTV (Linear Time Varying) equations. Pluym and Damaren[24] improved Ross's[25] results by expanding them to nonlinear equations with second-order J_2 gravity and the third-order spherical gravity. Schweighart and Sedwick[30] firstly developed linearized J_2 model in circular orbits. The gradient of the J_2 potential is used to calculate the in-plane relative motion, somewhat similar with Hill's equations. Mean variation in orbital elements and spherical trigonometry were employed to derive cross-track motion. Equations to describe this direction of motion are LTV and rather complicated. In order to simplify cross-track motion equations, Tillerson and How[34] established this motion by another method by incorporating the work of Vadali et al.[37] Recently, Xu and Wang[40] obtained a novel nonlinear direct ODE model, which considers all three aspects of error sources(nonlinearity, eccentricity and J_2 perturbation) and was derived based on Lagrange mechanics. And also this marks latest work in the search for a precise satellite relative motion.

3.2 Dynamic Models

3.2.1 Hill's Equations (HCW model)

Satellite formation flying designs can be derived from the linearized equations of relative motion for two objects under the influence of a point-mass gravitational field. Here, one object, which is called reference or chief satellite, is located at the origin of the LVLH coordinate system. Another, which is our research concern, is called deputy satellite . Hill's equations describe the relative motion of deputy satellites with respect to a reference satellite. Vallado[38] provides a detailed derivation of Hill's equations that take the following form:

$$\ddot{x} = 2n\dot{y} + 3n^2x \tag{3.1}$$

$$\ddot{y} = -2n\dot{x} \tag{3.2}$$

$$\ddot{z} = -n^2z \tag{3.3}$$

Where n is the angular velocity of the reference satellite. And here x, y and z represent position in radial, in-track, cross-track directions in LVLH coordinate respectively with respect to the reference satellite.
Three major assumptions are inherent in Hill's equations:

(1) The reference satellite traverses in a circular orbit;

(2) The distance between the objects is small in comparison to their orbital radius to justify simplification;

(3) No orbital perturbations are considered in these equations.

Based on HCW model, the paper by Sabol et al[26] gives a brief overview of the evolution of formation design and proposes several different types of formations

and their potential applications. The analytical solutions to Hill's equations are

$$x(t) = \frac{\dot{x}_0}{n}\sin nt - \left(3x_0 + \frac{2\dot{y}_0}{n}\right)\cos nt + 4x_0 + \frac{2\dot{y}_0}{n} \quad (3.4)$$

$$y(t) = \frac{2\dot{x}_0}{n}\cos nt + \left(6x_0 + \frac{4\dot{y}_0}{n}\right)\sin nt - (6nx_0 + 3\dot{y}_0)t - \frac{2\dot{x}_0}{n} + y_0 \quad (3.5)$$

$$z(t) = \frac{\dot{z}_0}{n}\sin nt + z_0\cos nt \quad (3.6)$$

where x_0, y_0, z_0 denote initial position and $\dot{x}_0$,$\dot{y}_0$,$\dot{z}_0$ represent initial velocity in three directions respectively. Note that (3.4) and (3.5) are coupled and secular growth term ($(6nx_0 + 3\dot{y}_0)t$) exists in the second equation. To avoid secular growth, we can set the secular term to zero by the constraint

$$\dot{y}_0 = -2x_0 n \quad (3.7)$$

This constraint provides the basis of formation flying design and initial conditions of deputy satellites. By substituting this initial condition into the analytical solutions, it can be proved that the motion in the radial/in-track plane will be a fixed point or an ellipse with the major axis in the in-track direction that is twice the minor axis in the radial direction. In this paper four formation designs are verified[26]. They are

- In-Plane Formation

  The formation consists of a set of deputy satellites occupying the same orbital plane and separated by mean anomaly. This formation is achieved by setting all initial conditions in Hill's equations, except for y_0, to zero. The primary advantage of in-plane formation is its simplicity in design, deployment, and

control.

$$x(t) = 0 \tag{3.8}$$

$$y(t) = y_0 \tag{3.9}$$

$$z(t) = 0 \tag{3.10}$$

where $y_0 \neq 0$ represents the amount of in-plane spacing between two satellites. This can be related to the mean anomaly separation[26] by

$$\Delta M = y_0/a \tag{3.11}$$

a denotes the semi-major axis of the satellite orbit.

- In-Track Formation

  In in-track formation design, all deputy satellites share the same ground track. For this formation, the solution to Hill's equations are

$$x(t) = 0 \tag{3.12}$$

$$y(t) = -y_0 \tag{3.13}$$

$$z(t) = -\frac{\omega_e}{n} y_0 \sin i \cos nt \tag{3.14}$$

  where ω_e is the rotation rate of the Earth, i is inclination. The attractiveness of in-track formation is each satellite in the formation passes over the same exact spots on the ground, which is valuable for Earth sensing.

- Circular Formation

  The circular formation is one in which deputy satellites maintain a constant distance from each other. The constraint of this formation is

$$x^2 + y^2 + z^2 = r^2 \tag{3.15}$$

where r is the radius of the formation. By substituting this constraint and (3.7) to (3.4)-(3.6), initial conditions can be obtained as:

$$\dot{y}_0 = -2nx_0 \tag{3.16}$$
$$y_0 = \frac{2\dot{x}_0}{n} \tag{3.17}$$
$$z_0 = \pm\sqrt{3}x_0 \tag{3.18}$$
$$\dot{z}_0 = \pm\sqrt{3}\dot{x}_0 \tag{3.19}$$

The circular formation has two properties that make it attractive: the satellites maintain a constant distance from each other and unlike the in-plane and in-track formations, the circular formation presents a three-dimensional array.

- Projected Circular Formation

  The projected circular formation only maintains a fixed distance the in-track and cross-track (y/z) plane. When the ellipse of relative motion is projected onto the y/z plane, it produces a circle. The constraint is

$$y^2 + z^2 = r^2 \tag{3.20}$$

By the analytical solution to Hill's equations, the initial conditions for this formation also can be derived as follows:

$$\dot{y}_0 = -2nx_0 \tag{3.21}$$
$$y_0 = 2\dot{x}_0/n \tag{3.22}$$
$$z_0 = \pm 2x_0 \tag{3.23}$$
$$\dot{z}_0 = \pm 2\dot{x}_0 \tag{3.24}$$

where the first two conditions set the along-track drift and offset to zero. The primary advantage of the projected circular formation is that the satellites are separated by a fixed distance when the formation is projected onto the

along-track/cross-track plane. This characteristic has applications for ground observing missions.

Yeh and Sparks[41] utilized Hill's equations to present some geometrical relationship for satellites in formation and by parameterizing Hill's equations, they provide insights into stable relative orbit for deputy satellites, which one is possible and which one cannot be designed.

3.2.2 TH Model

Inalhan and How[15] proved in their paper that chief orbit eccentricity has great effect on relative motion. Using Hill's equations, and considering chief orbit eccentricity $e = 0.005$ for typical shuttle orbit results in large consumption of fuel to maintain formation. Tschauner and Hempel[35] presented a method to derive the linearized relative dynamics with respect to an eccentric orbit via a unique set of elements and their time rate of change. The major assumptions of the derivation are

(1) Chief satellite orbit is elliptical;

(2) Distance between each satellites is small;

(3) No perturbation is included.

In the true anomaly domain, the eccentricity of chief satellite orbit can be naturally introduced. And the linear time varying equations can be written as

$$\frac{d}{d\theta}\begin{bmatrix} x' \\ x \\ y' \\ y \end{bmatrix}_j = \begin{bmatrix} \frac{2e\sin\theta}{1+e\cos\theta} & \frac{3+e\cos\theta}{1+e\cos\theta} & 2 & \frac{-2e\sin\theta}{1+e\cos\theta} \\ 1 & 0 & 0 & 0 \\ -2 & \frac{2e\sin\theta}{1+e\cos\theta} & \frac{2e\sin\theta}{1+e\cos\theta} & \frac{e\cos\theta}{1+e\cos\theta} \\ 0 & 0 & 1 & 0 \end{bmatrix}_j \begin{bmatrix} x' \\ x \\ y' \\ y \end{bmatrix}_j \quad (3.25)$$

$$+\frac{(1-e^2)^3}{(1+e\cos\theta)^4 n^2}\begin{bmatrix}1&0\\0&0\\0&1\\0&0\end{bmatrix}\begin{bmatrix}f_x\\f_y\end{bmatrix}_j \quad (3.26)$$

$$\frac{d}{d\theta}\begin{bmatrix}z'\\z\end{bmatrix}=\begin{bmatrix}\frac{2e\sin\theta}{1+e\cos\theta}&\frac{-1}{1+e\cos\theta}\\1&0\end{bmatrix}_j\begin{bmatrix}z'\\z\end{bmatrix}_j+\frac{(1-e^2)^3}{(1+e\cos\theta)^4 n^2}\begin{bmatrix}1\\0\end{bmatrix}f_z \quad (3.27)$$

where they use $(\bullet)'$ (such as x', $y'$and z' in above equations) to differentiate true anomaly domain from time domain. θ is true anomaly, f_x, f_y, f_z represent disturbances and control inputs in three directions. j denotes the jth satellite in the formation. Moreover, initial conditions that produce periodic solutions, preventing satellites drifting apart were derived. Under condition of argument of perigee $\omega = 0$, in true anomaly domain at perigee

$$\frac{y'(0)}{x(0)} = -\frac{2+e}{1+e} \quad (3.28)$$

If transformed to time domain

$$\frac{\dot{y}(0)}{x(0)} = -\frac{n(2+e)}{(1+e)^{1/2}(1-e)^{(3/2)}} \quad (3.29)$$

Here $\dot{y} = dy/dt$ is in time domain and $y' = dy/d\theta$ is expressed in true anomaly domain. The solution to the elliptical linearized equations are then compared to Hill's equations, and errors incurred by utilizing Hill's equations are presented. Due to the difficulty in solving the true anomaly domain LTV equations, Melton proposed another expression of the model by transforming these LTV equations into time domain as follow:

$$\ddot{x} = \frac{2\mu}{r^3}x + 2\omega\dot{y} + \dot{\omega}y + \omega^2 x \quad (3.30)$$

$$\ddot{y} = \frac{-\mu}{r^3}y - 2\omega\dot{x} - \dot{\omega}x + \omega^2 y \quad (3.31)$$

$$\ddot{z} = \frac{-\mu z}{r^3} \tag{3.32}$$

where $\omega = \dot{\theta} = \frac{n(1+e\cos\theta)^2}{1-e^2)^{3/2}}$, $\dot{\omega} = \ddot{\theta} = \frac{-2n^2 e\sin\theta(1+e\cos\theta)^3}{(1-e^2)^3}$, $r = \frac{a(1-e^2)}{(1+ecos\theta)}$. We can solve these differential equations using numerical method to predict relative motion with respect to elliptical chief orbit. Based on this dynamic model, Melton[22] expanded the state transition matrix in powers of eccentricity, while retaining the explicit time dependence of the three-dimensional motion.

3.2.3 Schweighart and Sedwick Model

Schweighart and Sedwick[30][31] from MIT developed a new set of constant-coefficient, linearized, differential equations to capture the the relative motion between satellites under J_2 perturbation. The major assumptions of derivation are

(1) The chief satellite orbit is circular;

(2) Distance between each satellites is small;

(3) Only J_2 perturbation is considered.

These equations are extensions of Hill's equations, and thus, they are similar to the representation of HCW model. The equations of motion can be written as

$$\ddot{x} - 2(nc)\dot{y} - (5c^2 - 2)n^2 x = 0 \tag{3.33}$$

$$\ddot{y} + 2(nc)\dot{x} = 0 \tag{3.34}$$

$$\dot{\gamma} - nb\cos\gamma = 0 \tag{3.35}$$

$$\dot{\Phi} - nb\Phi\cos\gamma\sin\gamma = 0 \tag{3.36}$$

where $z = r_{ref}\Phi\sin(knt - \gamma)$. γ is angular distance between the equator and the intersection of two orbital planes (chief and deputy orbit). Φ represents maximum angular cross-track separation. The solutions to the differential equations of motion are

$$x = x_0\cos(gnt) + (g/2c)y_0\sin(gnt) \tag{3.37}$$
$$y = -(2c/g)x_0\sin(gnt) + y_0\cos(gnt) \tag{3.38}$$
$$z = r_{ref}\Phi\sin(knt - \gamma) \tag{3.39}$$
$$\Phi = \Phi_0(\cos\gamma_0)(\sec\gamma) \tag{3.40}$$
$$\gamma = \tan^{-1}(bnt + \tan\gamma_0) \tag{3.41}$$

The initial conditions are

$$\dot{x}_0 = (ny_0/2)(g^2/c) \tag{3.42}$$
$$\dot{y}_0 = -2cnx_0 \tag{3.43}$$
$$\dot{z}_0 = (k-b)nr_{ref}\Phi_0\cos(\gamma_0) \tag{3.44}$$
$$z_0 = r_{ref}\Phi_0\sin(-\gamma_0) \tag{3.45}$$
$$\Phi_0 = (1/r_{ref})\sqrt{z_0^2 + [\dot{z}_0/(k-b)n]^2} \tag{3.46}$$
$$\gamma_0 = -a\tan^{-2}\{[\dot{z}_0/n(k-b)], z_0\} \tag{3.47}$$

and the constants are

$$j = (3J_2R_e^2)/2r_{ref}^2 \tag{3.48}$$
$$n = \sqrt{\mu/r_{ref}^3} \tag{3.49}$$
$$s = j[(1 + 3\cos 2i_{ref})/4] \tag{3.50}$$
$$b = j\sin^2 i_{ref} \tag{3.51}$$

$$k = c + j\cos^2 i_{ref} \tag{3.52}$$

$$c = \sqrt{1+s} \tag{3.53}$$

$$g = \sqrt{1-s} \tag{3.54}$$

3.2.4 Tillerson and How Model

Tillerson and How[34] used a modified dynamic model which combines the work of Schweighart and Sedwick model and Vadali[37]. The major assumptions of deriving the model are

(1) Chief satellite orbit is circular;

(2) Distance between each satellites is small;

(3) Only J_2 perturbation effects is included.

This dynamic model can be written as

$$\ddot{x} = 2nc\dot{y} + (5c^2 - 2)n^2 x \tag{3.55}$$

$$\ddot{y} = -2nc\dot{x} \tag{3.56}$$

$$\ddot{z} = -(3c^2 - 2)n^2 z + 2Anca_{ref}\cos\alpha\sin\theta_{ref} \tag{3.57}$$

with $s = \frac{3}{8}J_2\left(\frac{R_{earth}}{a_{ref}}\right)^2(1+3\cos(2i_{ref}))$
$c = \sqrt{s+1}$ $A = \frac{3}{2}J_2 n\left(\frac{R_{earth}}{a_{ref}}\right)^2\sin^2(i_{ref})\frac{\rho}{a_{ref}}$
where n is the mean motion, a_{ref} is the semi-major axis, i_{ref} is the inclination, and θ_{ref} is the true anomaly of the reference orbit. α is the formation phasing angle and ρ is the formation size. Though the assumption and expression of Tillerson and How model and Schweighart and Sedwick model are similar, we can find that for cross-track motion, J_2 disturbance is modeled in two different ways. Schweighart

and Sedwick employed mean variation in orbit elements and spherical trigonometry to derive cross-track motion. While in Vadali's work[37], J_2 disturbance is modeled as an input disturbance. So the final expression for cross-track motion are different.

Furthermore, there are two reasons to develop Tillerson and How model. First, for in-plane dynamics, Vadali's model[37] requires complicated indirect calculation to obtain parameters whereas Schweighart and Sedwick model provides a direct calculation for the parameter to achieve the same effect. And second, for out of plane motion, Schweighart and Sedwick model requires several calculation involving both relative and absolute measurements to determine the disturbance, whereas Vadali model[37] only requires a relatively straightforward calculation. Therefore, to some extend, Tillerson and How model, a combination, may give the best fit to the nonlinear orbital simulation.

Based on this dynamic model, Tillerson and How presented advanced formation-keeping guidance algorithm that use linear programming to determine fuel-optimal control inputs and state trajectories.

3.2.5 Unperturbed Nonlinear Model

Vaddi et al [36] derived a system of nonlinear differential equations. They are widely used in formation design, to minimize error caused by linearization and eccentricity. The effect of eccentricity of chief satellite orbit, which influences the relative motion dynamics of the deputy are captured by the augmented fourth-order dynamics of the chief. The equations can be written as

$$\ddot{x} - 2\omega\dot{y} - \omega^2 x = -\frac{\mu(r_c + x)}{[(r_c + x)^2 + y^2 + z^2]^{3/2}} + \frac{\mu}{r_c^2} \tag{3.58}$$

$$\ddot{y} + 2\omega\dot{x} + \dot{\omega}x - \omega^2 y = -\frac{\mu y}{[(r_c + x)^2 + y^2 + z^2]^{3/2}} \tag{3.59}$$

$$\ddot{z} = -\frac{\mu z}{[(r_c + x)^2 + y^2 + z^2]^{3/2}} \tag{3.60}$$

$$\ddot{r_c} = r_c\omega^2 - \frac{\mu}{r_c^2} \tag{3.61}$$

$$\dot{\omega} = -\frac{2\dot{r_c}\omega}{r_c} \tag{3.62}$$

where x, y and z are the relative motion coordinates of the deputy with respect to the chief in the LVLH frame. r_c refers to the radius of the chief satellite from the center of the Earth. $\omega = \dot{\theta}$, θ refers to the latitude angle of the chief, and μ is the gravitational parameter. The major assumption of deriving this model is only

(1) No orbital perturbation is considered.

Gurfil[12] obtains initial condition of this model guaranteeing bounded motion between any two satellites on arbitrary Keplerian elliptic orbits as follows

$$\begin{aligned}&\tfrac{1}{2}\{(\dot{x}_0 - \dot{\theta}_0 y_0 + \dot{r}_{c0})^2 + [\dot{y}_0 + \dot{\theta}_0(x_0 + r_{c0})]^2 + \dot{z}_0^2\} \\ &\quad -\mu/\sqrt{(r_{c0} + x_0)^2 + y_0^2 + z_0^2} = -\mu/2a_c\end{aligned}$$

where a_c is semi-major axis of chief satellite.

3.2.6 Xu-Wang Model

In the latest development on satellite formation flying, Xu and Wang[40] recently derived a satellite relative dynamic model which includes chief orbit eccentricity, nonlinearity and J_2 perturbation. The major assumption of derivation of this new model is only

(1) No orbital perturbations except J_2 is considered.

Their paper presents a set of nonlinear ordinary differential equations for the satellite relative motion based on Lagrangian Mechanics. Accurate J_2 dynamics of chief orbit are considered to ensure precise relative dynamics with respect to the chief orbit. Their model is composed of two parts: one is to desribe reference orbit dynamics and the other is to capture the relative motion. These equations are:

$$\ddot{x} = 2\dot{y}\omega_z - x(n_j^2 - \omega_z^2) + y\alpha_z - z\omega_x\omega_z - \Delta\zeta \sin i \sin\theta - r(n_j^2 - n^2) \quad (3.63)$$

$$\ddot{y} = -2\dot{x}\omega_z + 2\dot{z}\omega_x - x\alpha_z - y(n_j - \omega_z^2 - \omega_x^2) + z\alpha_x - \Delta\zeta \sin i \cos\theta \quad (3.64)$$

$$\ddot{z} = -2\dot{y}\omega_z - x\omega_x\omega_z - y\alpha_x - z(n_j^2 - \omega_x^2) - \Delta\zeta \cos i \quad (3.65)$$

where ω_x, α_x,α_z, n^2, n_j^2, $\Delta\xi$ are variables given by

$$\omega_x = -\frac{k_{J2}}{r^5\omega_z}(\sin 2i \sin\theta) \quad (3.66)$$

$$\alpha_x = -\frac{k_{J2}}{r^5}(\sin 2i \cos\theta) + \frac{3\nu_\gamma k_{J2}}{r^6\omega_z}(\sin 2i \sin\theta) \quad (3.67)$$

$$-\frac{2k_{J2}^2}{r^{10}\omega_z^2}\sin^2 i \sin 2i \sin 2\theta \sin\theta \quad (3.68)$$

$$\alpha_z = -\frac{2\omega_z\nu_\gamma}{r} - \frac{k_{J2}}{r^5}(\sin^2 i \sin 2\theta) \quad (3.69)$$

$$n^2 = \frac{\mu}{r^3} + \frac{k_{J2}}{r^5} - \frac{5k_{J2}}{r^5}\sin^2 i \sin^2\theta \quad (3.70)$$

$$n_j^2 = \frac{\mu}{r_j^3} + \frac{k_{J2}}{r_j^5} - \frac{5k_{J2}r_{jZ}^2}{r_j^7} \quad (3.71)$$

$$\Delta\zeta = \frac{2k_{J2}r_{jZ}}{r_j^5} - \frac{2k_{J2}}{r^4}(\sin i \sin\theta) \quad (3.72)$$

where ν_γ, r, θ, i, ω_z are solutions of dynamics of reference orbit as follows

$$\dot{r} = \nu_\gamma \quad (3.73)$$

$$\dot{\nu_\gamma} = \omega_z^2 - \frac{\mu}{r^2} - \frac{k_{J2}}{r^4}(1 - 3\sin^2 i \sin^2\theta) \quad (3.74)$$

$$\dot{\theta} = \omega_z + \frac{2k_{J2}}{r^5\omega_z}(\cos^2 i \sin^2\theta) \tag{3.75}$$

$$\dot{i} = -\frac{k_{J2}}{2r^5\omega_z}(\sin 2i \sin 2\theta) \tag{3.76}$$

$$\dot{\omega}_z = -\frac{2\omega_z\nu_\gamma}{r} - \frac{k_{J2}}{r^5}(\sin^2 i \sin 2\theta) \tag{3.77}$$

parameters k_{J2}, r_{jZ}, and r_j are defined as

$$k_{J2} = \frac{3J_2\mu R_e^2}{2} \tag{3.78}$$

$$r_j = \sqrt{(r+x)^2 + y^2 + z^2} \tag{3.79}$$

$$r_{jZ} = r\sin i \sin\theta + x \sin i \sin\theta + y \sin i \cos\theta + z\cos i \tag{3.80}$$

It is stated in the paper[40] that this dynamic model does not have model error in arbitrary eccentric orbits under J_2 perturbation. So these equations can be used to propagate the satellite relative motion from the specified initial conditions. Also, the orbital energy matching condition, which matches chief and deputy satellite orbital energy to prevent drifting, is given by:

$$2\mu\left(\frac{1}{r_j} - \frac{1}{r}\right) = (\dot{r} + \dot{x}_j - y_j\omega_z)^2 - \dot{r}^2 + (r\omega_z + \dot{y}_j + x_j\omega_z)^2 - r^2\omega_z^2 + \dot{z}_j^2 \tag{3.81}$$

By satisfying this condition, we can construct a bounded relative motion between chief and deputy satellites.

Chapter 4

Comparison Study of Models

4.1 Objective

In general, the accuracy of a relative motion model is correlated to its complexity. Thus, an important question is which model is appropriate for a given problem or which factors need to be included in dynamic model. The objective of model comparison studied in this thesis consists of two parts. One is to evaluate impact of different perturbation effects on the development of relative motion theories. The other is to compare model accuracy under near practical orbital environment. These will provide valuable insights into dynamic models of satellite relative motion and facilitate subsequent formation design and fuel-optimal control development.

There are numerous dynamic models in the literature. In the thesis, we focus only on direct ODE models for comparison, because they are more amenable for controller design. The comparison method and model error index proposed in this thesis can also be used to evaluate other categories of models.

In section 4.2, firstly we propose a framework for comparison of various dynamic models. Comparison study is based on simulation using simulation platform STK.

The key features of STK and the reason for its adoption for our satellite formation flying research will be stated. With the assistance of STK and Matlab, a demonstration of how to study initial conditions in the scenario of formation initialization will be illustrated, including introduction to simulation in STK and STK & Matlab interface. Finally, the model error index, which will be used to evaluate various dynamic models in this thesis, will be presented.

4.2 Model Comparison Method

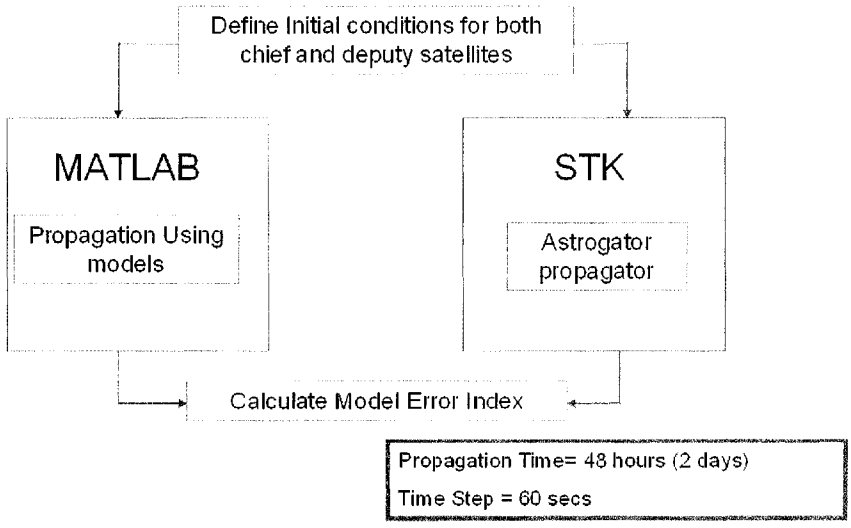

Figure 4.1: Function Chart of Model Comparison Method

In our study, we need a satellite motion propagator, which is precise, standard, and acceptable in practical application to predict future satellites orbit. Then all the theories prediction can be compared with that propagator. In this research, we choose STK as a standard propagator for our simulation platform. The reason for using STK will be stated in the following section in details. Figure 4.1 shows function chart of model comparison method.

(1) As the first step, we will define a group of initial conditions for chief and

deputy satellites, including initial positions and velocities.

(2) In the next step, we utilize the STK-Matlab interface to transfer these data into STK Astrogator.

(3) Then the same initial conditions will be propagated in both STK and Matlab independently. Relative motion predictions of different models are numerically generated by solving differential equations using Matlab toolbox ode45. For STK, we can customize the propagator to include various orbital perturbations.

(4) Through interface, satellites orbit data generated will be collected in Matlab and coordinate conversion is carried out. Finally the model error index is calculated.

All dynamic models under study will be subjected to the same test set-up and benchmarked to STK.

4.3 Simulation Platform

Because our comparison study is based on simulation, the accuracy of simulation tool will directly affect our final results, especially for evaluation purposes. Therefore, to choose a high fidelity and widely acceptable simulation platform is critical for our comparison study.

There are many satellite simulation tools, such as Quicksat[2], Satellite Tracker[4], Freeflyer[1], etc. All of them are designed to generate predictions for satellite's orbit. Some of them are for special applications, some designed for general purpose. The complexities of these modeling platforms are very different, the simplest one run in DOS, and the most sophisticated one consists of more than twenty modules and databases. Our selected simulation platform STK (Satellite Tool Kit)[3] is

one of the most popular and successful commercial satellite analytical software widely used in industries and academics. STK performs complex analysis of space missions in one integrated solution. Its functionality enables users to calculate position and orientation, evaluate inter-visibility times, and determine quality of dynamic spatial relationships. Here are some key features of STK:

- Integrated 2-D and 3-D visualization
- Complex vehicle propagation models, such as Aircraft Mission Modeler and High-Fidelity Orbit Propagator(HFOP)
- Define custom geometries, vectors, coordinate systems, and reference frames
- Inter-visibility analysis including complex and custom constraining conditions, group intervisibility, and chained inter-visibility
- Complex sensor modelling
- Custom data product generation, including reports, graphs and Visual Data Format Files
- Data exchange with other software such as Matlab, and has programmable interface
- Professional authoring capabilities
- Webcast for near real-time, distributed visualization via internet or local network
- Industry-standard image support
- Terrain analysis and visualization

In contrast to other satellite related software, several features of STK are very important for the accuracy of our simulation. For example, HFOP provide accurate

orbit propagation. It uses a semi-numerical method to generate satellite orbit, which is based both on solving differential equations and using multiple databases to correct the solutions each time step. Programmable interface allows us to design our control part in Matlab and share the data between STK and Matlab to implement the control strategy in near future. And other features greatly facilitate our experiment. For instance, we can define our own coordinate in STK, since formation coordinate is different from normal coordinate such as inertial or body-fixed frame commonly used in spacecraft design. 2-D and 3-D visualization and custom data production generation provide us a flexible tool to process the data and report. That's why we choose STK as our simulation platform.

4.4 Simulation in STK

Next, we will briefly introduce how we run simulation in STK. Following is a demonstration of how to simulate relative motion of chief and deputy satellites in STK.

4.4.1 Creation of a Scenario

In this demonstration, chief satellite orbit properties are set in accordance with low Earth orbit mission as table 4.1 below.

Chief Satellite Orbit	Value
Semi-major axis	$7000km$
Inclination	$20°$
Eccentricity	0
Other Orbital Elements	0

Table 4.1: Orbital elements of chief satellite

In STK environment we set these data into chief satellite orbit initial state block, see Figure 4.2. In Figure 4.2, Coord.System includes Earth Inertial, Earth Fixed,

Earth PseudoFixed and so on. Element type includes Cartesian, Keplerian, Modified Keplerian, Spherical, Target Vector Incoming Asymptote and so on.

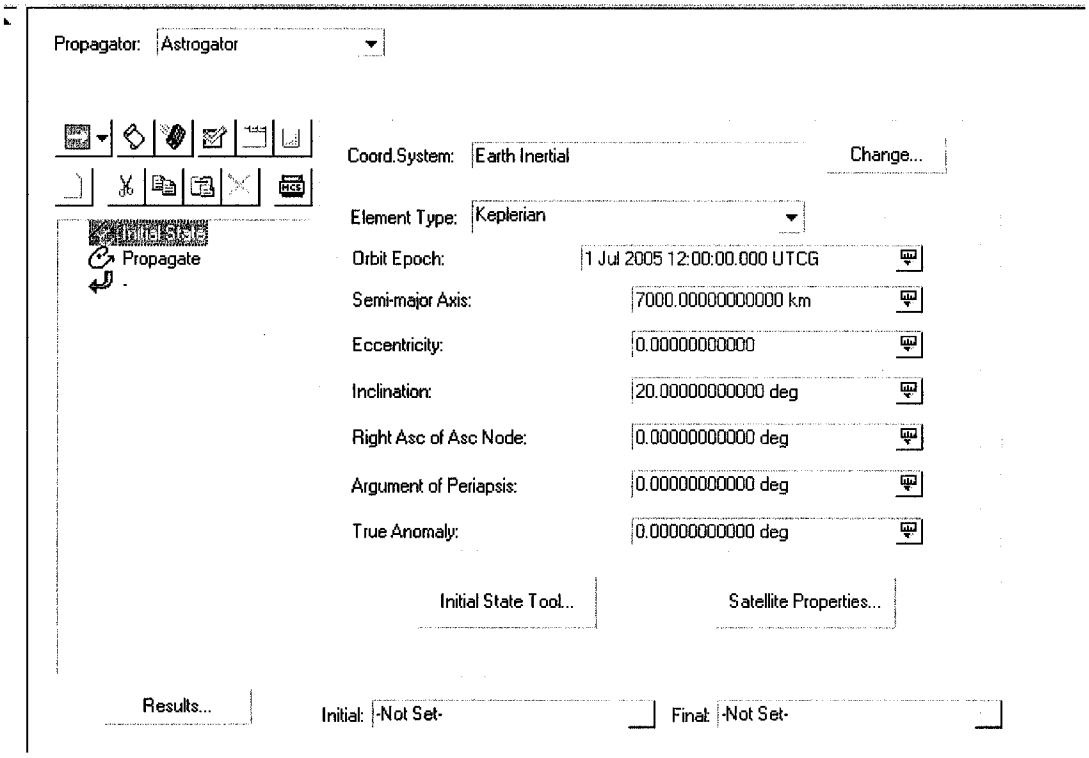

Figure 4.2: STK Astrogator Orbit Initial State

For deputy satellite, we can set its initial conditions in the same way as the chief but need to define its reference vehicle, as shown in Figure 4.3.

In this demonstration, the initial conditions of deputy satellite are adjusted according to Hill's equations, as shown in table 4.2 below.

Relative Position and Velocity	Value
x	$0.1km$
y	0
z	0
$\dot{x}$	0
$\dot{y}$	$-0.0002156km/s$
$\dot{z}$	0

Table 4.2: Relative Position of Deputy Satellites

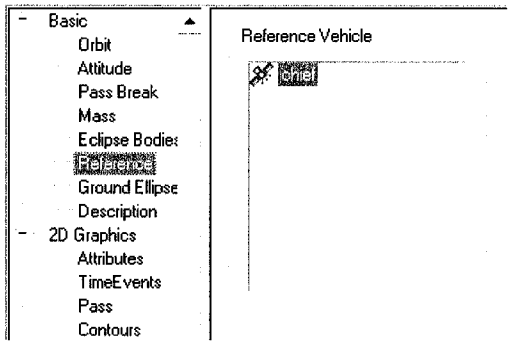

Figure 4.3: Set Deputy Satellite Reference Vehicle

Figure 4.4 shows how to configure satellite parameters. We use STK default satellite settings: satellite dry mass is $500kg$, drag coefficient is equal to 2.2, and drag area is $1e-006km^2$.

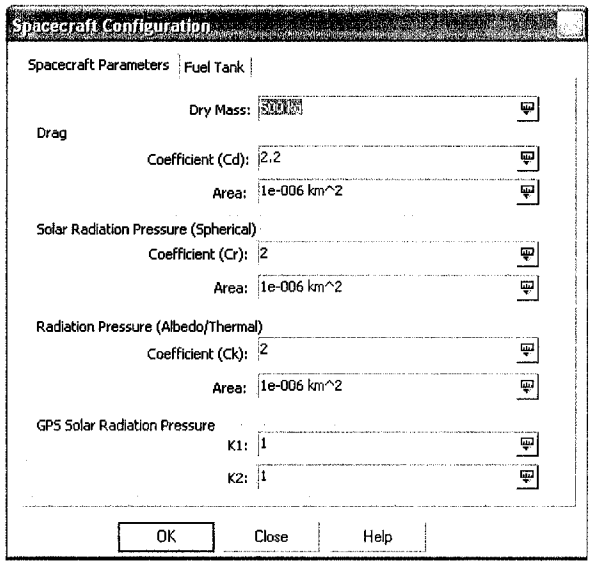

Figure 4.4: Satellite Parameters Configuration

4.4.2 Selection of Propagator

In order to evaluate models under different orbital perturbations we need to customize the propagator in STK. Figure 4.5 shows STK Astrogator propagator con-

figuration. We can customize our propagator to include orbital perturbations such as J_2, J_4... solar radiation pressure, atmospheric drag, third body gravity and so on. Or we can simply use STK predefined propagators such as Earth full, Earth J_2, Earth point mass propagator.

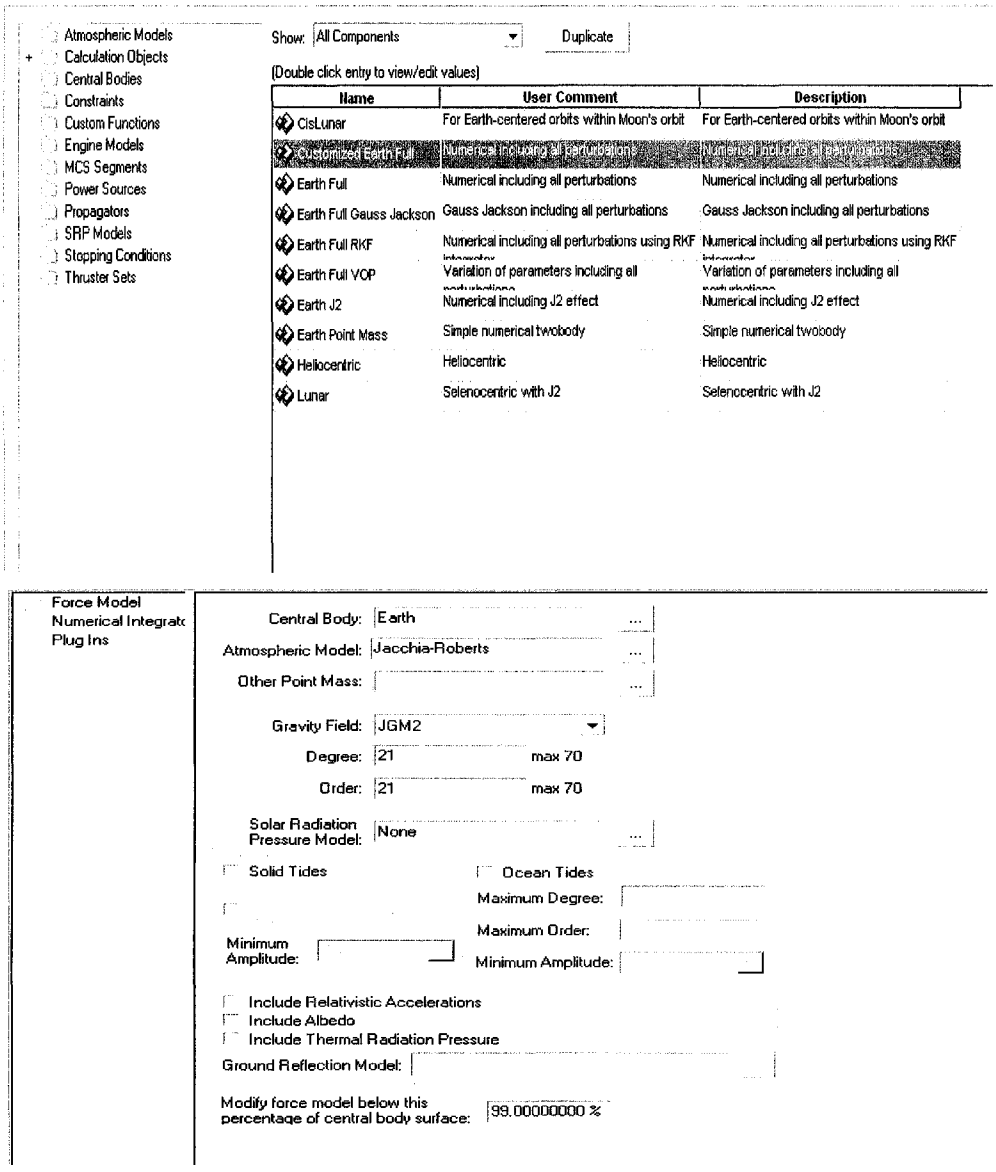

Figure 4.5: STK Astrogator Propagator Configuration

4.4.3 Data Processing

Once we define the scenario and propagator, we can generate satellite absolute and relative motion in STK automatically. STK provides various tools for data processing and collecting. You can export the data into files for further processing or you can real-time transport data to another program. STK has its own graphic tools, which can plot data simultaneously. Figure 4.6 , which is generated by STK graphic tool, shows the relative motion between the predefined chief and deputy satellite.

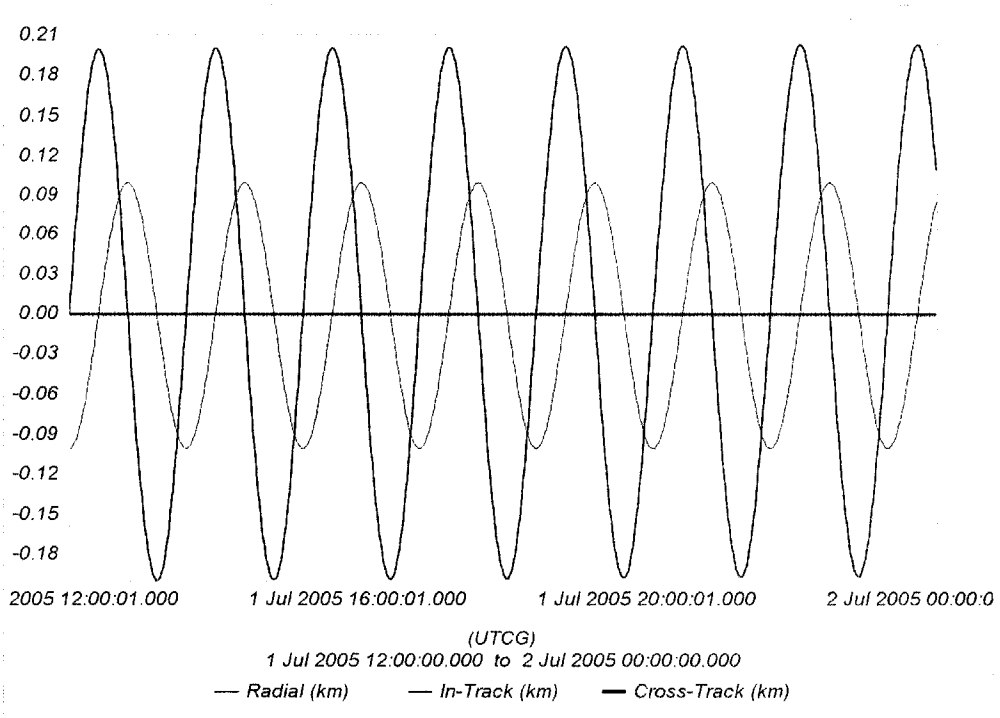

Figure 4.6: Relative Motion between Chief and Deputy Satellite Plotted by STK

4.5 Interface of STK and Matlab

Because we run most of our computation in Matlab and high precision propagation in STK, we need a interface to exchange data between STK and Matlab. STK

provides its own Matlab interface. It is composed of two parts. One is called "aerotoolbox", including functions for orbital mechanics computation. The other one is called "mexconnect", which consists of commands for Matlab Client/STK Server communication.

In Matlab, we firstly use command "agiinit" and "stkinit" to initialize the interface. Following commands are used to transfer chief satellite initial states to STK Astrogator.

```
%transfer chief orbit initial conditions to STK
conComd=['ASTROGATOR /Scenario/NTU/Satellite/chief SETVALUE
MainSEQUENCE.SegmentList.Initial_State.InitialState.Keplerian.sma ',num2str(a,12),'
km'];
stkexec(conID,conComd);
conComd=['ASTROGATOR /Scenario/NTU/Satellite/chief SETVALUE
MainSEQUENCE.SegmentList.Initial_State.InitialState.Keplerian.ecc ',num2str(e,12)];
stkexec(conID,conComd);
conComd=['ASTROGATOR /Scenario/NTU/Satellite/chief SETVALUE
MainSEQUENCE.SegmentList.Initial_State.InitialState.Keplerian.inc ',num2str(i,12),'
deg'];
stkexec(conID,conComd);
conComd=['ASTROGATOR /Scenario/NTU/Satellite/chief SETVALUE
MainSEQUENCE.SegmentList.Initial_State.InitialState.Keplerian.RAAN
',num2str(Omega,12),' deg'];
stkexec(conID,conComd);
conComd=['ASTROGATOR /Scenario/NTU/Satellite/chief SETVALUE
MainSEQUENCE.SegmentList.Initial_State.InitialState.Keplerian.w ',num2str(w,12),'
deg'];
stkexec(conID,conComd);
conComd=['ASTROGATOR /Scenario/NTU/Satellite/chief SETVALUE
MainSEQUENCE.SegmentList.Initial_State.InitialState.Keplerian.TA
',num2str(nu,12),' deg'];
stkexec(conID,conComd);
```

Keywords "conComd" contains Astrogator commands. "stkexec" transfers these commands to STK and executes them. Command "ASTROGATOR/..../ SETVALUE ..." is used to set values for STK Astrogator scenarios.

Command "stkPropagate" is for initiating propagation in STK. After propagation, following commands are used to transfer data back to Matlab and organize them.

```
% Propagate deputy satellite and transfer the relative position data from
% STK to Matlab

stkPropagate('/Scenario/NTU/Satellite/deputy',0,43200);
[Data,Name]=stkreport('/Scenario/NTU/Satellite/deputy','RelativeMotion-position');
stk_relpos_x=stkfinddata(Data{1},'Radial')/1000;
stk_relpos_y=stkfinddata(Data{1},'InTrack')/1000;
stk_relpos_z=stkfinddata(Data{1},'CrossTrack')/1000;
stk_relpos_vx=stkfinddata(Data{1},'RadialRate')/1000;
stk_relpos_vy=stkfinddata(Data{1},'InTrackRate')/1000;
stk_relpos_vz=stkfinddata(Data{1},'CrossTrackRate')/1000;
```

Command "stkreport" returns a array, which contains Astrogator object values. Command "stkfinddata" is used to collect and organize data from the array to Matlab.

4.6 Model Error Index

In order to evaluate various dynamic models accuracy in our simulation platform, a model error index is required to objectively compare different models. K. T. Alfriend and H. Yan[5] proposed a nonlinear index for comparing the accuracy of various dynamic models. Their method is based on Junkins et al.[16] nonlinear index for comparing linear theories. Here we propose a simple index for comparison in the simulation. Our model error index σ is described in this way:

$$\sigma = \frac{1}{n}\sum_{i=1}^{n} \log_2(1 + P_i^{(e)})(1 + V_i^{(e)})^w \tag{4.1}$$

where

$$V_i^{(e)} = \cos^{-1}\left(\frac{\vec{v}_i^{STK} \bullet \vec{v}_i^{M}}{|\vec{v}_i^{STK}||\vec{v}_i^{M}|}\right) \tag{4.2}$$

$$P_i^{(e)} = \frac{|\vec{r}_i^{STK} - \vec{r}_i^{M}|}{\rho} \tag{4.3}$$

$\vec{v}^{STK_i}$, $\vec{v}_i^M$ are velocity vectors and $\vec{r}_i^{STK}$, $\vec{r}_i^M$ are position vectors. Here, data generated by STK and Matlab are with superscript "STK" and "M" respectively. n denotes total steps. i denotes the ith step. $P_i^{(e)}$ and $V_i^{(e)}$ represent the position and velocity difference between STK and dynamic model prediction.

Actually, in (4.2), $V_i^{(e)}$ is an adjusted radian value between two velocity vectors. It can effectively indicate model error caused by relative orbit rotation which was called tumbling in previous chapters. The exponent w is a weighted value which can be used to adjust $V_i^{(e)}$ in line with $P_i^{(e)}$. Increasing w would lead to rotation effect playing greater role in our model index and vice versa. In the following chapter simulation, $w = 2$ is carried out in the experiment to weigh equally the error caused by relative orbit rotation and drift.

Note that the above model error index is computed at each time point of satellite orbit with identical time step. This index is proportional to model error, thus, the smaller the index, the more accurate the model is.

Chapter 5

Model Error Study: Perturbation Effects

5.1 Simulation Scenario

For perturbation effects on model error, the errors caused by chief orbit eccentricity, J_2 disturbance and atmospheric drag are studied in this chapter. Table 5.1 describes three typical and widely used dynamic models, which are analyzed under differential perturbations in our simulation platform. In Table 5.1, $\surd$ and X denotes whether a perturbation is considered in the derivation of the respective dynamic model. For HCW model, we simulate formation initialization and incorporate perturbations from J_2 to Earth full disturbance, which will prove that other disturbances(except orbital eccentricity and J_2) have little effects on formation flying. For TH model and Schweighart and Sedwick model, we find that their results are better for compensating impact of orbit eccentricity and J_2 effect, respectively.

Disturbances	HCW Model	TH model	Schweighart and Sedwick model
Eccentricity	X	$\surd$	X
J_2 effect	X	X	$\surd$

Table 5.1: Comparison study formulation

Here, we use a chief and a deputy satellite with $0.1km$ radial separation case as our simulation scenario. Two cases of orbital elements of chief satellite, which is simulated in the platform, are shown in table 5.2 below.

Chief Satellite	Case 1	Case 2
Semi-major Axis	$7000km$	$7000km$
Inclination	45°	45°
Eccentricity	0	0.005
Other Orbital Elements	0	0

Table 5.2: Orbital parameters of chief satellite

The initial velocities of deputy satellites are adjusted according to different models, See Section 3.2. All the linearized models are simulated both in STK and Matlab. In STK, we customize the Astrogator propagator to adopt different disturbances to evaluate the impact of various perturbations. For every model, formation relative orbit is generated in Matlab by solving the differential equations. The initial conditions are applied into STK propagator to generate the "real" orbit. Model error is calculated every time step 60s(Model error=STK results - Matlab results). The scenario duration time is 86400 seconds(24 hours).

5.2 Simulation Results and Discussion

5.2.1 Orbit Eccentricity

One important assumption made in HCW model is that the chief satellite travels in a circular orbit. Actually, most spacecraft orbits are elliptical. Figure 5.1 shows the HCW model error when the reference orbit is an ellipse with a very little eccentricity $e = 0.005$. We can see that the model error gets larger and larger. After 24 hours propagation, the model error associated with in-track direction is more than $0.4km$. That makes HCW model no longer applicable.

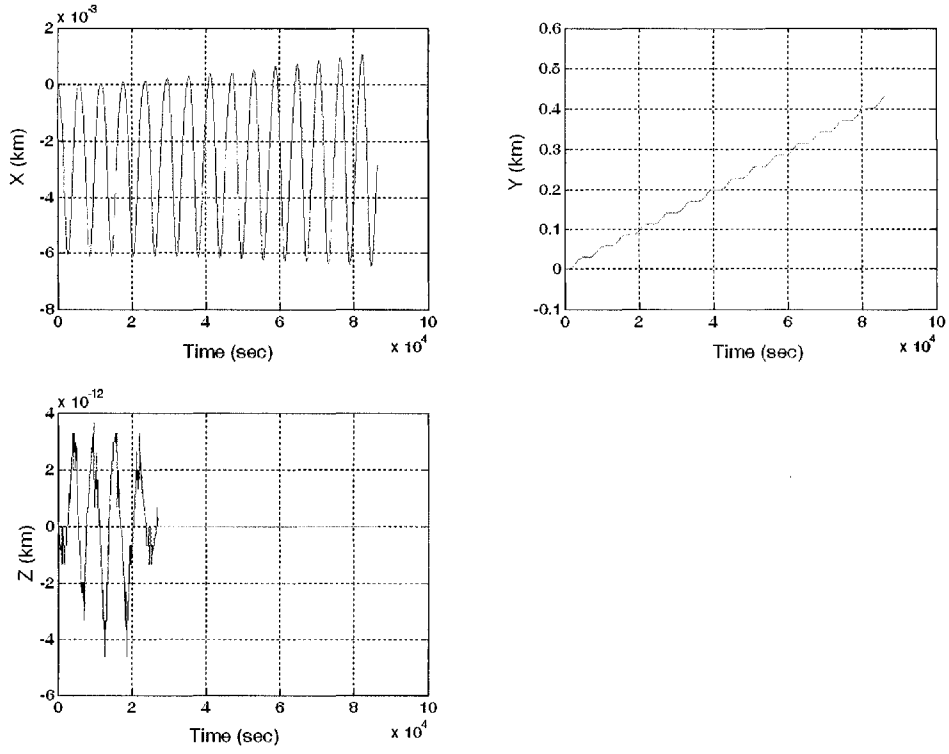

Figure 5.1: HCW Model Error with Small Chief Orbit Eccentricity 0.005

In order to improve the dynamic model performance in such eccentric chief orbit condition, Tschauner and Hempel[35] developed a new dynamic model in true anomaly and time domain. Inalhan and How[15] presented a set of initial conditions for this model to apply in formation flying in their paper.(see section 3.2.2) In our simulation, deputy satellite initial velocity is adjusted according to their derivation (3.2.20) and (3.2.21) ($\dot{y}_0 = -0.000217229 km/s$).

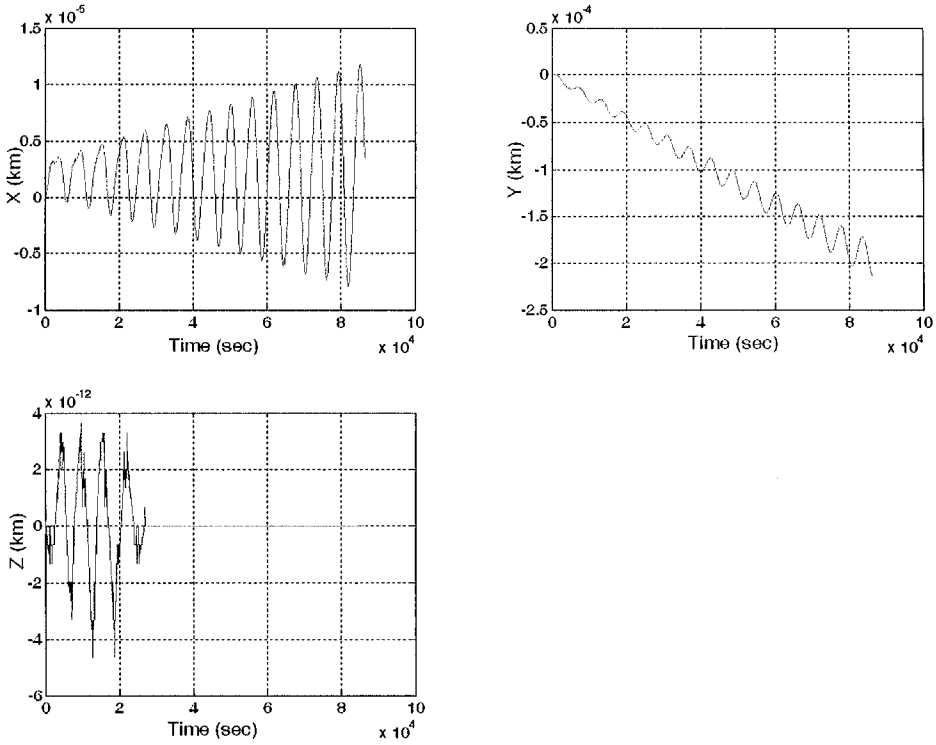

Figure 5.2: TH Model Error with Chief Orbit Eccentricity 0.005

Figure 5.2 shows the simulation results using TH model in time domain. In contrast to Figure 5.1, model error in both radial and in-track direction decreases.

Remark 5.1: In contrast to HCW model, TH model greatly improves the model accuracy when chief orbit is elliptic. Therefore TH model is better for capturing relative motion when reference orbit eccentricity is considered. In addition, we find that in-track velocity is very sensitive to the formation stability, because the difference between HCW and TH model velocity adjustment is very small.

5.2.2 J_2 Disturbance

Figure 5.3 shows HCW model error when incorporate J_2 disturbance during a period of 24 hours. Although deputy satellite initial velocity has been adjusted by Hill's equations, motions in three directions is no longer periodical, but fast drifting apart.

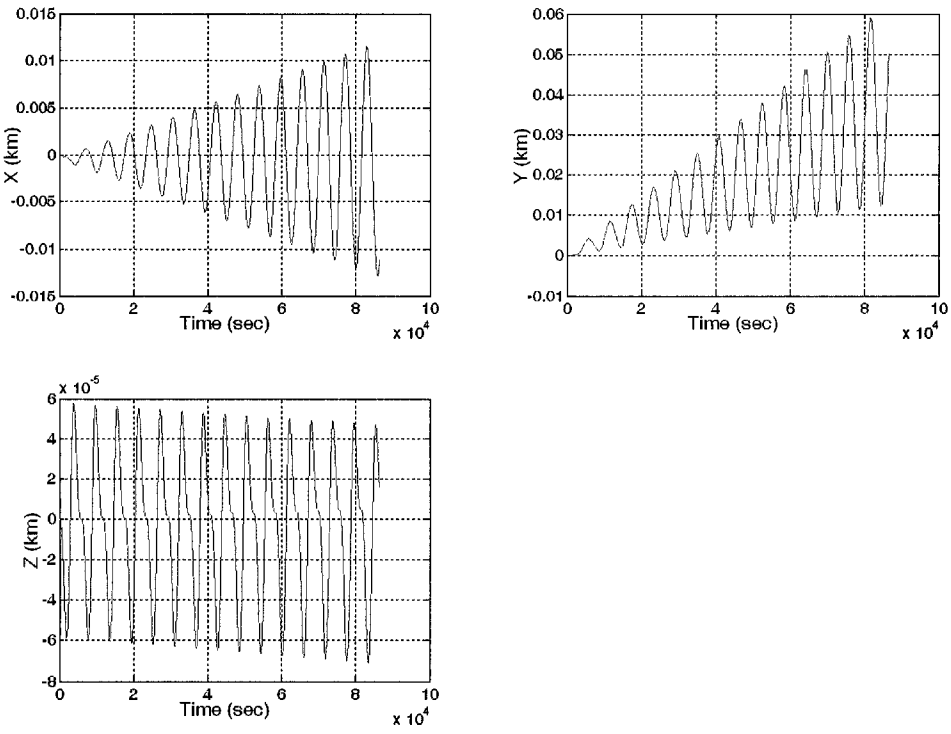

Figure 5.3: HCW Model Error under J_2 Perturbation

Though TH model can compensate model error caused by orbit eccentricity, Figure 5.4 shows that when J_2 effect is present, TH model error substantially increases. It is no longer able to construct stable formation. Another model should be developed to overcome J_2 impact.

Remark 5.2: TH model only can compensate error caused by chief orbit eccen-

tricity. It does not address J_2 effects.

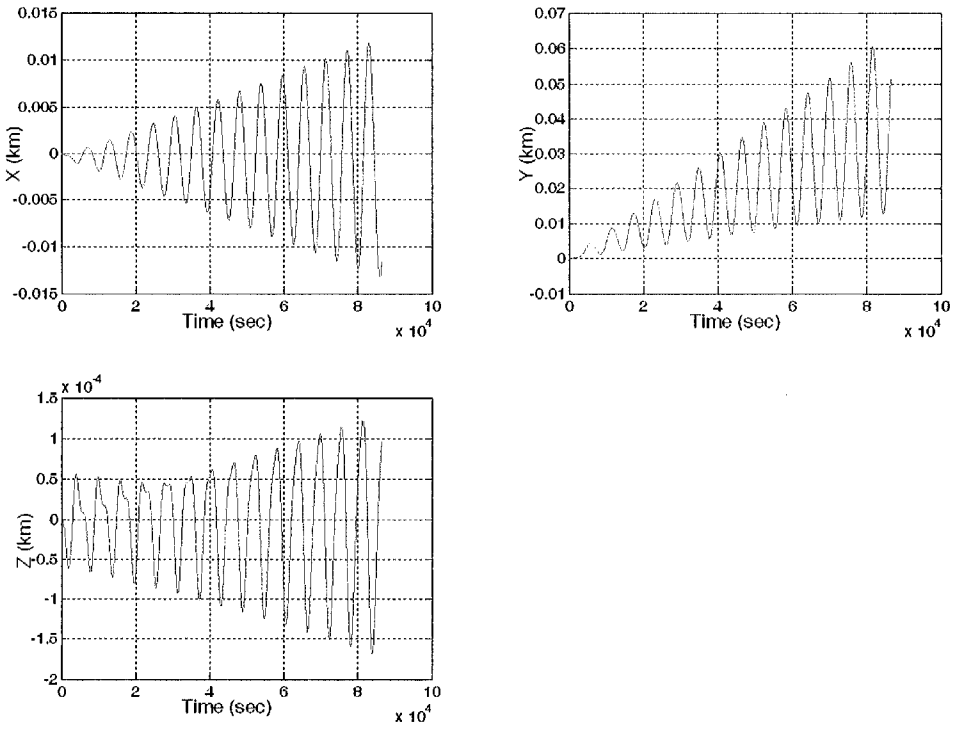

Figure 5.4: TH Model Error under J_2 Perturbation

Previous simulation shows J_2 perturbation gradually ruins the formation (shown in Figure 5.3 and Figure 5.4). Though the impact is not so great as ignoring eccentricity (see Figure 5.1), it is crucial for designing stable formations. In section 3.2.3, Schweighart and Sedwick's[30][31] J_2 model is stated. After initial conditions are adjusted in line with (3.36) and (3.37). We evaluate this model in STK and Matlab.

Figure 5.5 shows that using Schweighart and Sedwick model, model errors associated with radial and in-track directions are smaller in contrast to Figure 5.3 and Figure 5.4. The STK results are well predicted by this model. However, in cross-track direction, the model does not overcome slight drift. And in radial and in-track direction, the model error is not periodical but increasing although the

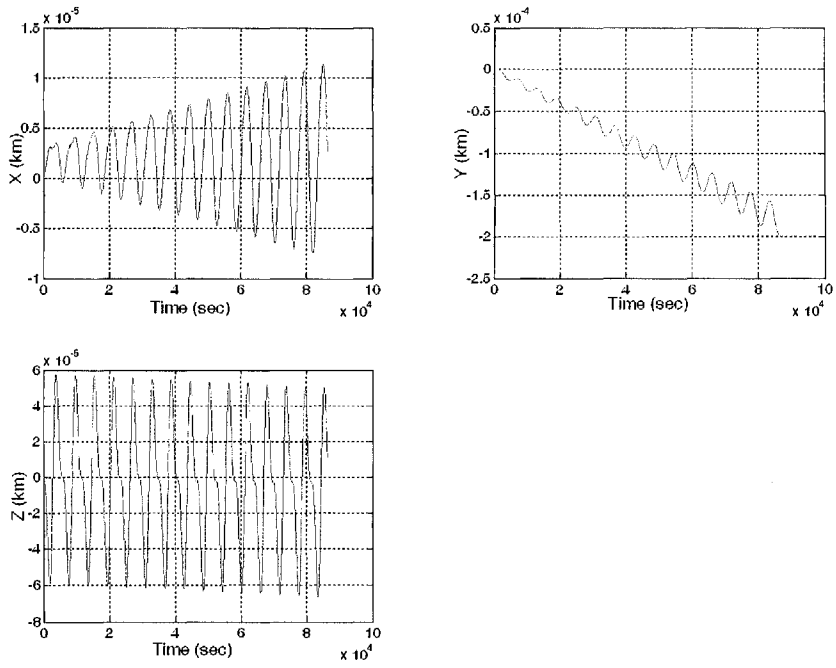

Figure 5.5: Schweighart and Sedwick Model Error under J_2 Perturbation

scale is small. This would lead to unstable formation in a long period.

Remark 5.3: By using Schweighart and Sedwick model, simulation results show that the model error associated is small but non-periodical. Therefore this model is better for capturing relative motion when J_2 effect incorporated. But Figure 5.6 also shows there is a slight error increment in all three directions. This will propagate over time and needs to be carefully monitored.

5.2.3 Atmospheric Drag and Solar Radiation

To evaluate atmospheric drag and solar radiation effects on satellites relative motion, we use simple HCW model. In Figure 5.6, HCW model error is shown with atmospheric drag and solar radiation effect added into STK propagator. Comparing with Figure 5.1, during 24 hours, the HCW model error does not have great

changes in all three directions. Therefore, atmospheric drag and solar radiation pressure has relatively smaller effects on satellite relative motion dynamics.

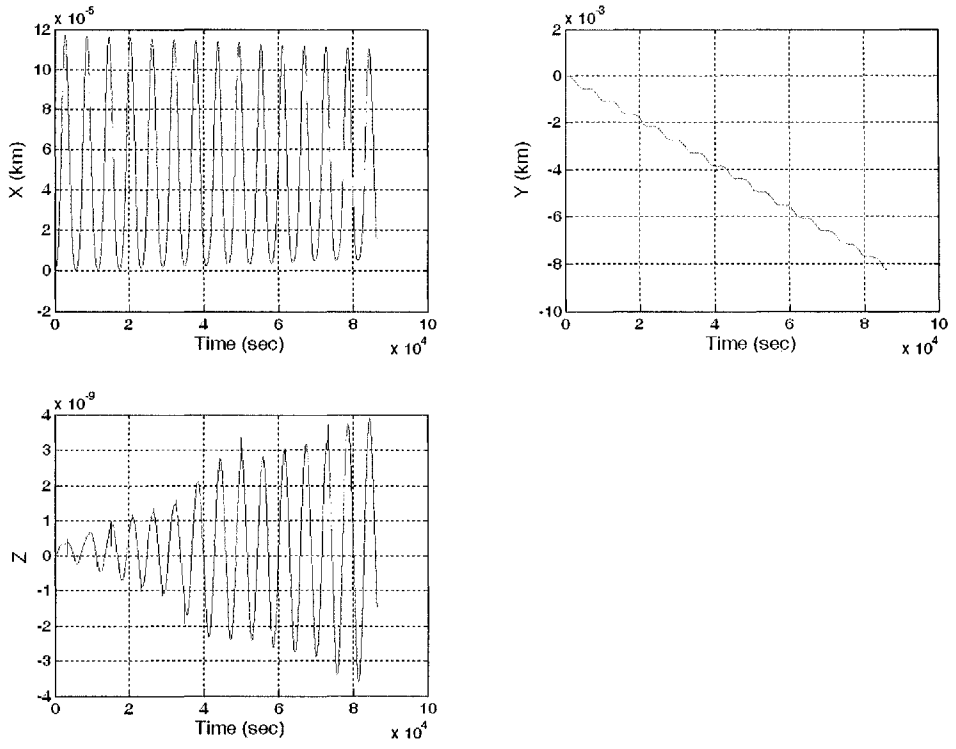

Figure 5.6: HCW Model Error under Atmospheric Drag and Solar Radiation Effect

Remark 5.4: When J_2 effect, atmospheric drag and solar radiation incorporated(see Figure 5.3 and Figure 5.6), Hill's equations cannot capture the relative motion between reference and deputy satellites. In addition, we can find that HCW model error caused by atmospheric drag and solar radiation is around 10^{-3} to 10^{-9} km in condition of $r(perigee) \geq 7000$ km. In contrast to J_2 effect($10^{-2} \sim 10^{-5}$ km), it is much smaller, and can be safely ignored.

Remark 5.5: Comparing Figure 5.1 with Figure 5.3 and Figure 5.6, we can find that Chief satellite orbit eccentricity dominates the differential disturbances. The second important factor is J_2 effect and the other disturbances effects are comparatively small.

Chapter 6

Model Error Study: Comparison

6.1 Simulation Scenario

We set up a projected circular orbit (PCO) in the LVLH frame centered at the chief satellite. It can be described by

$$x = 0.5\rho\sin(\theta + \alpha_0) \tag{6.1}$$

$$y = \rho\cos(\theta + \alpha_0) \tag{6.2}$$

$$z = \rho\sin(\theta + \alpha_0) \tag{6.3}$$

where θ is the true latitude angle of the chief satellite, ρ is the radial of PCO, α_0 is initial phase angle of orbit . we select four parameters i, e, a and ρ as variable for comparison in the simulation. Later, it will be proved that these four parameters have important effects on dynamic model accuracy.

In the next step, all dynamic models are simulated in Matlab. Relative motion predictions of the these models are numerically generated by solving differential equations using Matlab toolbox ode45. Meanwhile the same cases are also im-

plemented in STK, using customized STK Astrogator propagator, incorporating perturbations such as $J_2 ... J_{21}$ and atmospheric drag. Subsequently, data are transferred from STK to Matlab to calculate the model error index.

In the simulation, the test cases are defined in Table 6.1, Table 6.2 and Table 6.3:

Chief Satellite Orbit	Value
a	$6600 \sim 8000$ km
Ω	$0°$
i	$0 \sim 90°$
e	$1e-4 \sim 0.01$
ω	$0°$
v	$0°$

Table 6.1: Orbital Elements of Chief Satellite

Deputy Satellite Orbit	Value
x_0	$0.5\rho \sin\alpha_0$ km
y_0	$\rho \cos\alpha_0$ km
z_0	$\rho \sin\alpha_0$ km
$\dot{x}_0$	0 km/s
$\dot{y}_0$	adjusted by (3.64)
$\dot{z}_0$	0 km/s
α_0	$90°$
ρ	$0.10 \sim 20.0$ km

Table 6.2: Parameters of Deputy Satellite and Formation

Satellite Parameters	Value
Dry Mass	500 kg
Drag Coefficient	2.2
Drag Area	$1e-006\ km^2$

Table 6.3: Satellite Parameters Configuration

When the eccentricity of the chief orbit is not zero, the relative motion is similar to PCO. For all the cases, we use energy matching initial conditions (3.81) to prevent large drift in in-track direction. However, note that both approximate PCO formation and period matching conditions will not affect our evaluation and

comparison results. Because the dynamic model should be able to precisely predict future relative motion between satellites, no matter we test what kind of formation or whether the formation is stable. So does it in STK Astrogator propagator. Our objective is to calculate the model error index σ (4.1) for each dynamic model, through varying the eccentricity e, semi-major axis a, inclination of the chief satellite orbit i and PCO radius ρ. The duration of scenario is 24 hours , and the index is generated every 60 seconds (n=1440).

6.2 Simulation Results

6.2.1 Error Index vs Formation Size ρ

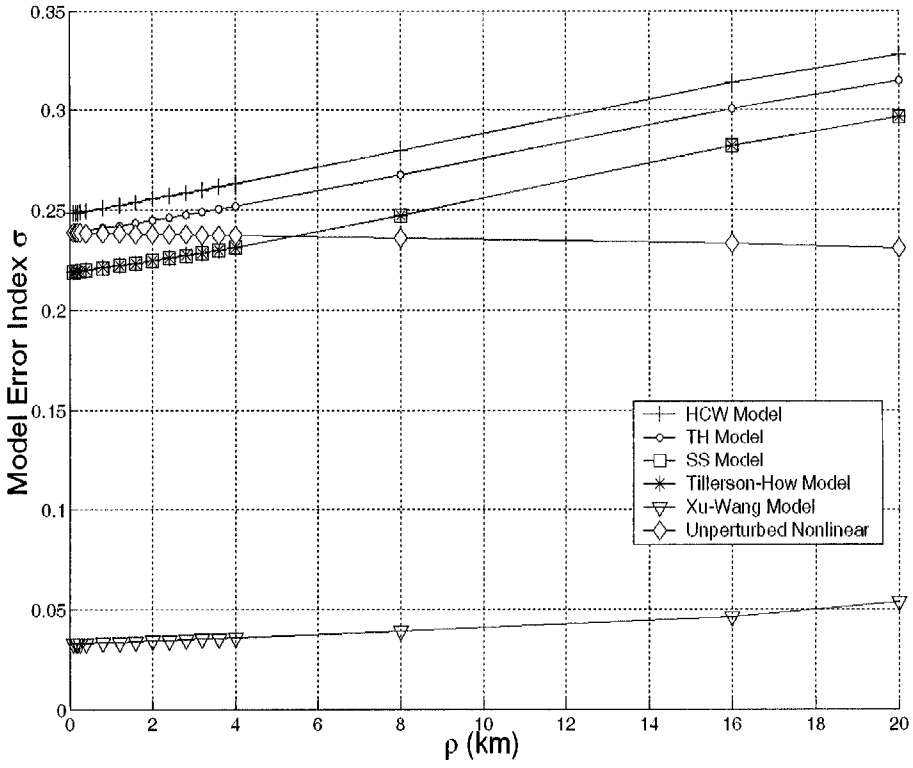

Figure 6.1: Index Comparison for $e = 0.0001$, $i = 45°$, $a = 6600km$

Figure 6.1-6.4 show the index comparison varying with the PCO radius for different chief orbit eccentricity and semi-major axis. Since our index is proportional to model error, the comparison provides a guideline for determining the model accuracy for specific problem and application. In Figure 6.1, as the eccentricity is approximately zero, and when the formation size is small, we find that the index of linearized models are small and close to each other. Models which are based on the assumption of circular chief orbit and which include J_2 effects, perform better for smaller formation size. When PCO radius is below $5.8km$, Schweighart and

Sedwick model and Tillerson-How model have the smallest error. However, when eccentricity of chief orbit increases, which is shown in Figure 6.3 and Figure 6.4, the performance of the models, which inlude chief orbit eccentricity, is better than the other models.

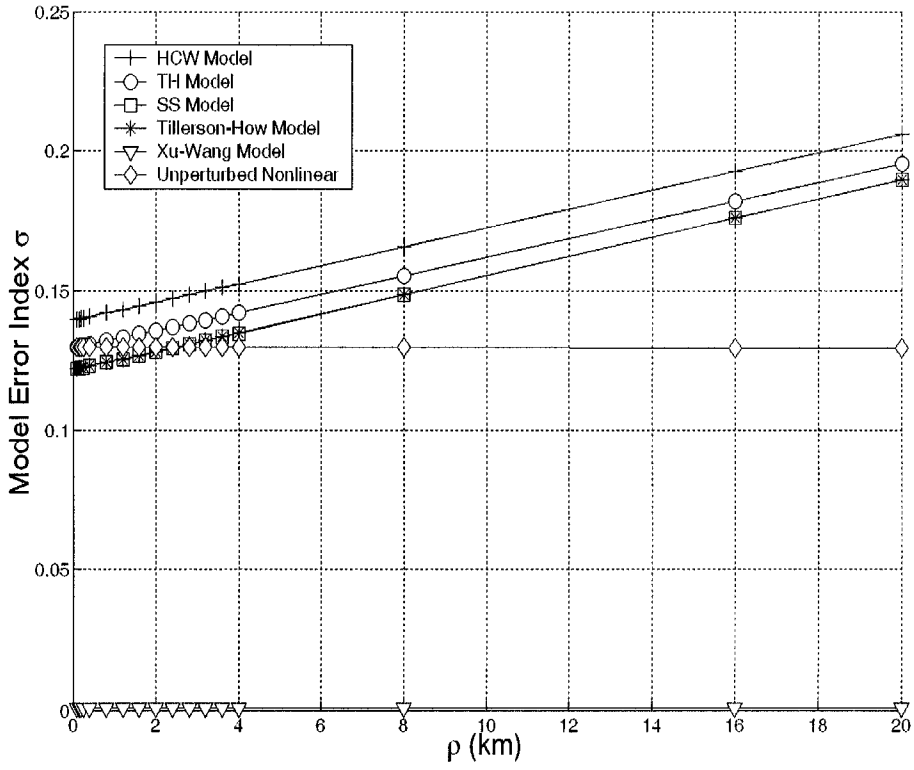

Figure 6.2: Index Comparison for $e = 0.0001$, $i = 45°$, $a = 8000km$

For the case of large chief orbit eccentricity, as shown in Figure 6.4, Xu-Wang model, TH model and unperturbed nonlinear model performed best. We can find that within 2 km PCO radius, error indexes of TH model and unperturbed nonlinear model are similar. Since TH model is linearized, for controller design under such condition, we recommend the use of TH model. Moreover, the above figures also show that when PCO radius become large, all linearized model errors increased. We should use nonlinear model when formation size is larger than 10 km. In other words, when formation size is larger than 10 km, the key factor

affecting model accuracy is nonlinearity. For consider, a specific mission with a satellite formation whose chief orbit is highly eccentric and the formation size is 15 km. Figure 6.3 and 6.4 show Xu-Wang model and unperturbed nonlinear model can perform well under such requirement. The model error difference between these two models is roughly constant. So depending on mission accuracy requirements, we can use Xu-Wang model for highly accurate design or use unperturbed nonlinear model for preliminary design.

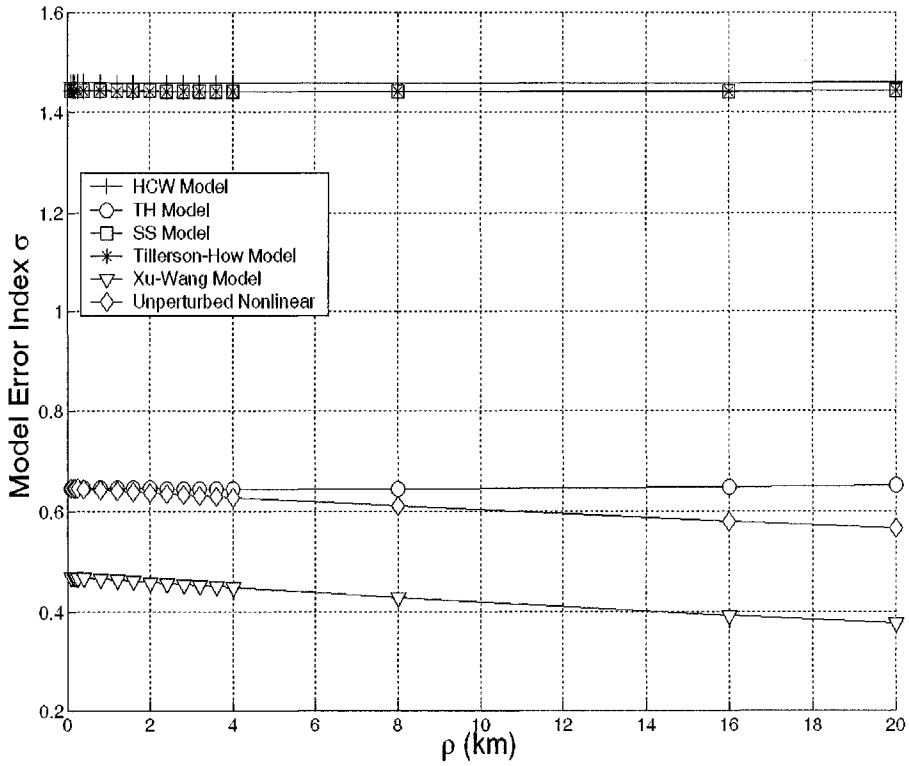

Figure 6.3: Index Comparison for $e = 0.01$, $i = 45°$, $a = 6600km$

The impact of atmospheric drag is related to the semi-major axis of chief satellite orbit. Comparing Figure 6.1 and 6.2, we can see that Xu-Wang model error increases, no longer close to zero, when chief orbit is low. That's the result of drag effects. Figure 6.3 and 6.4 also show the same result.

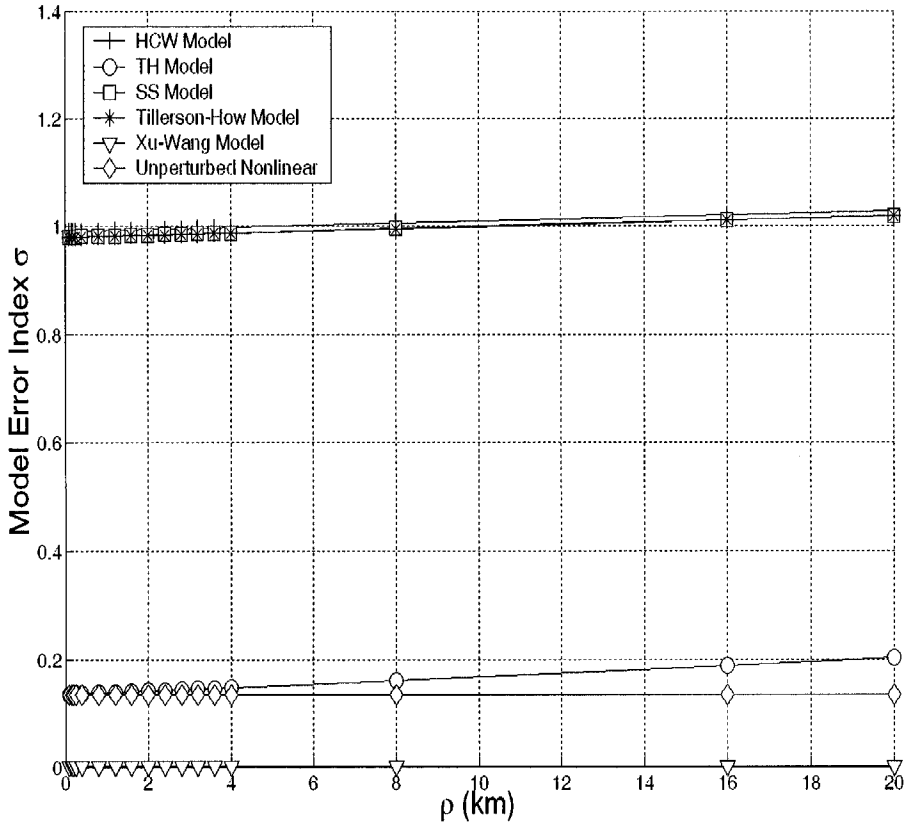

Figure 6.4: Index Comparison for $e = 0.01$, $i = 45°$, $a = 8000km$

6.2.2 Error Index vs Chief Orbit Eccentricity e

Figures 6.5-6.8 show the effect of error index as a function of chief orbit eccentricity for various formation size and semi-major axis. As the eccentricity gets larger, errors of three linear dynamic models (HCW model, Schweighart and Sedwick model, Tillerson-How model), which excludes eccentricity consideration, grow larger and larger. In contrast to index comparison with formation size variation, eccentricity changes lead to noticeable error growth for most of dynamic models. Thus chief orbit eccentricity is the dominant disturbance to satellite formation. Moreover, in Figure 6.5-6.8, the differences of index between unperturbed nonlinear model and Xu-Wang model show the benefits of modeling J_2 perturbation.

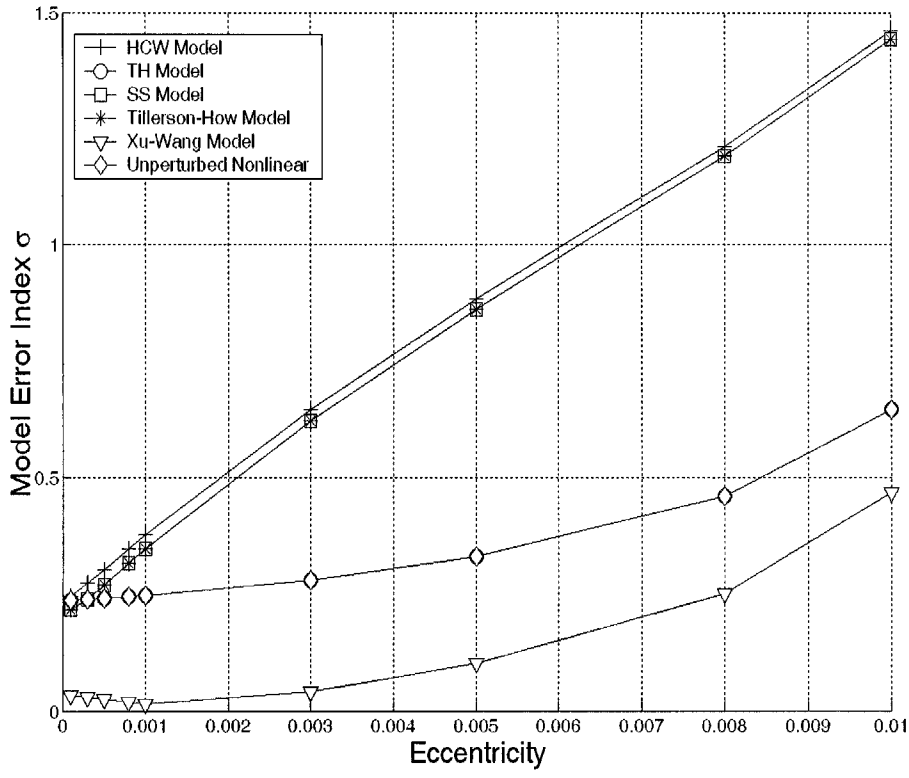

Figure 6.5: Index Comparison for $\rho = 0.1km$, $i = 45°$, $a = 6600km$

The index differences between TH model and unperturbed nonlinear model show effects of modeling nonlinearity. It grows as formation size increases. As shown in results, when the formation radius is less than 20 km, the impact of nonlinearity effects is less than J_2 effects. In Figure 6.5 and Figure 6.6, the performance of TH model and unperturbed nonlinear model is the same. That means we can ignore nonlinearity effects when formation size is small enough ($\rho = 0.1km$). Figure 6.5 and Figure 6.7 show that when chief satellite orbit is low, increasing eccentricity will lead to significant errors for all dynamic models, because satellites are greatly affected by atmospheric drag at perigee of highly eccentric orbit. Note that in Figure 6.5 and 6.7, error index of Xu-Wang model and TH model increases as chief orbit eccentricity increases. That is different from Figure 6.4 and 6.6, which is shown as constants. The reason of such difference is that we reduce the chief

orbit semi-major axis to 6600 km. At this low altitude, atmospheric drag effect plays an important role. We will study the details of the impact of atmospheric drag in Section 6.2.4.

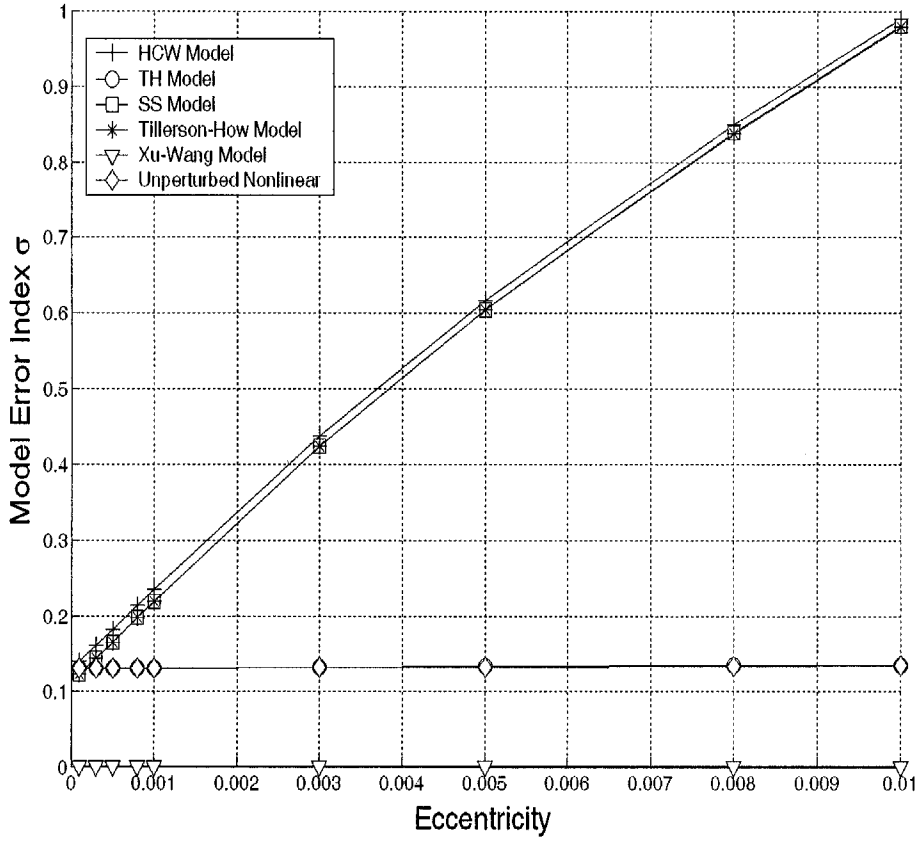

Figure 6.6: Index Comparison for $\rho = 0.1km$, $i = 45°$, $a = 8000km$

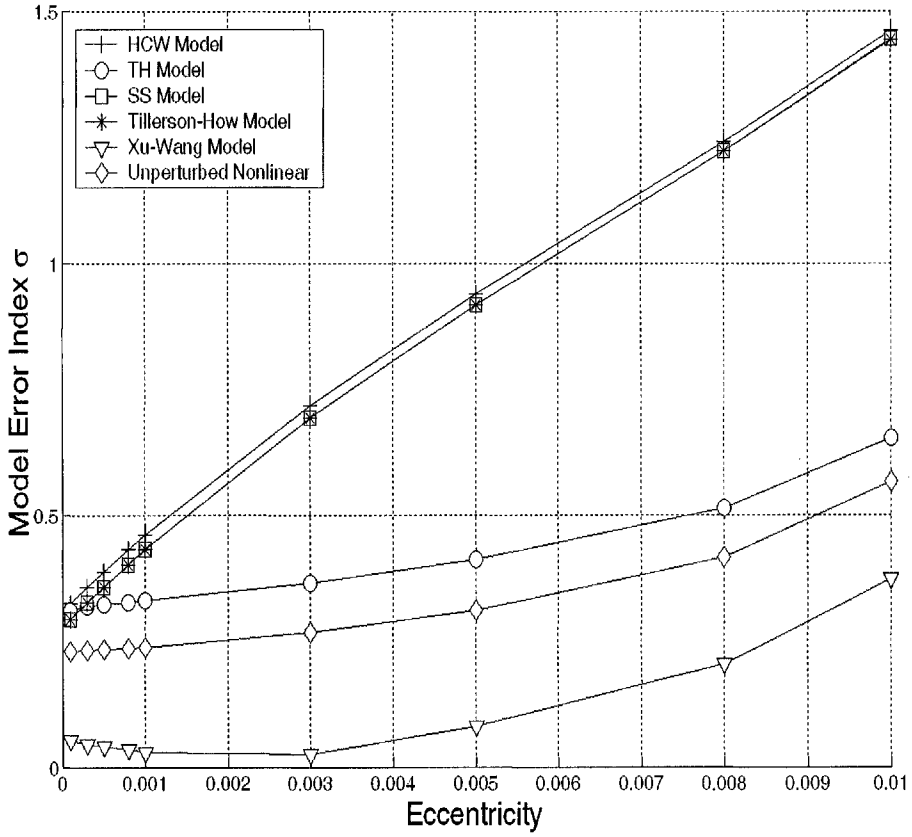

Figure 6.7: Index Comparison for $\rho = 20km$, $i = 45°$, $a = 6600km$

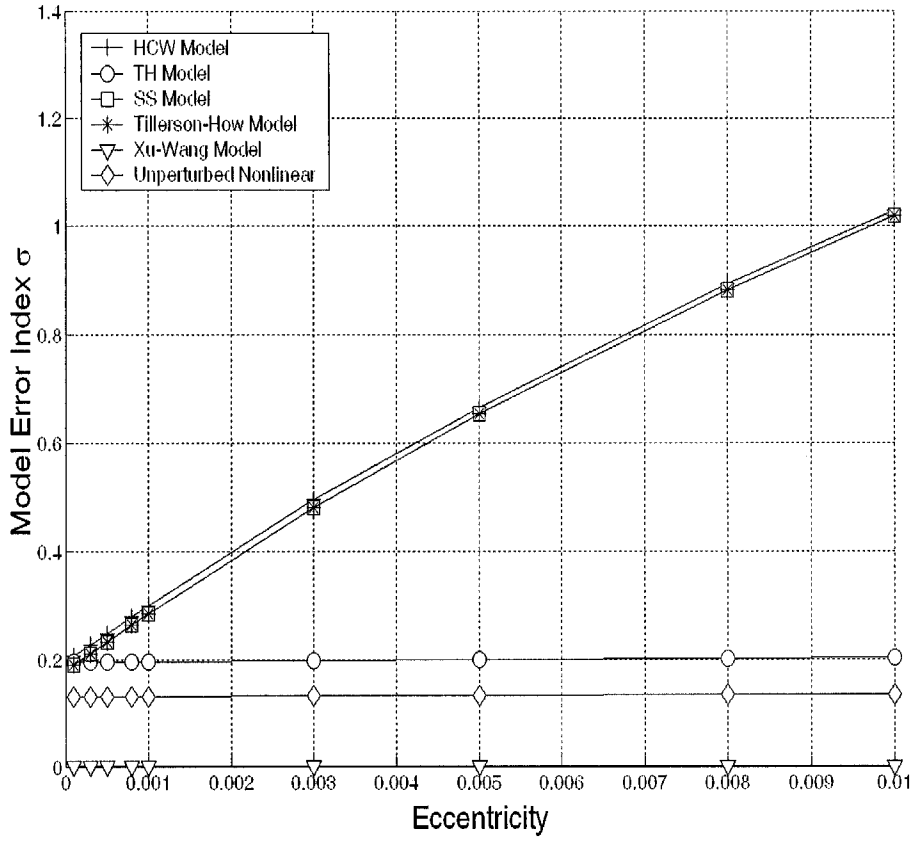

Figure 6.8: Index Comparison for $\rho = 20km$, $i = 45°$, $a = 8000km$

6.2.3 Error Index vs Chief Orbit Inclination i

Figures 6.9-6.12 show error index comparison as a function of chief orbit inclination for different eccentricity, PCO radius and semi-major axis, respectively. The simulation results show that Schweighart and Sedwick model and Tillerson-How model have distinct error trend. They seem more stable as inclination varies. For small inclinations, small eccentricity, and small formation radius, these two dynamic models outperform others except Xu-Wang model, see Figure 6.9 and Figure 6.12. In addition, there are several interesting intersections of Schweighart and Sedwick model, Tillerson-How model and the other three models in figures. These inter-

section points indicate that the different models have similar performance under the same conditions. When the chief orbit inclination is larger than 60 degrees, index comparison shows that the other four models are better than Schweighart and Sedwick model and Tillerson-How model. In summary, our simulation results demonstrate that nonlinearity (formation size), chief orbit eccentricity, semi-major axis and inclination are four key parameters for satellite formation flying mission design. All play important roles in our final dynamic model selection.

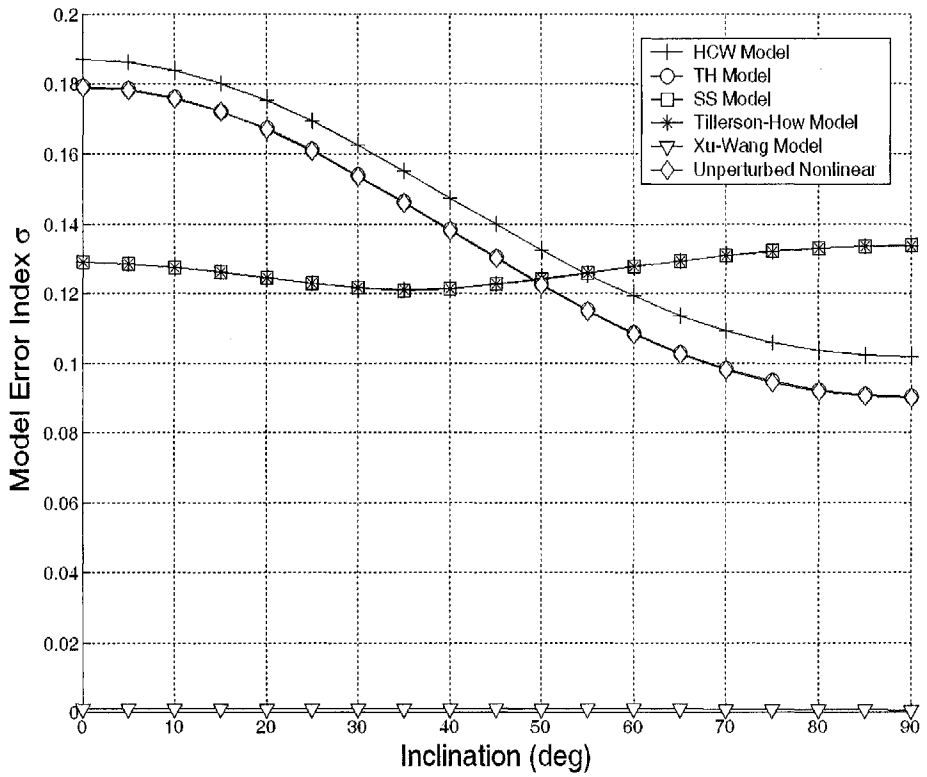

Figure 6.9: Index Comparison for $\rho = 0.1km$, $e = 0.0001$, $a = 8000km$

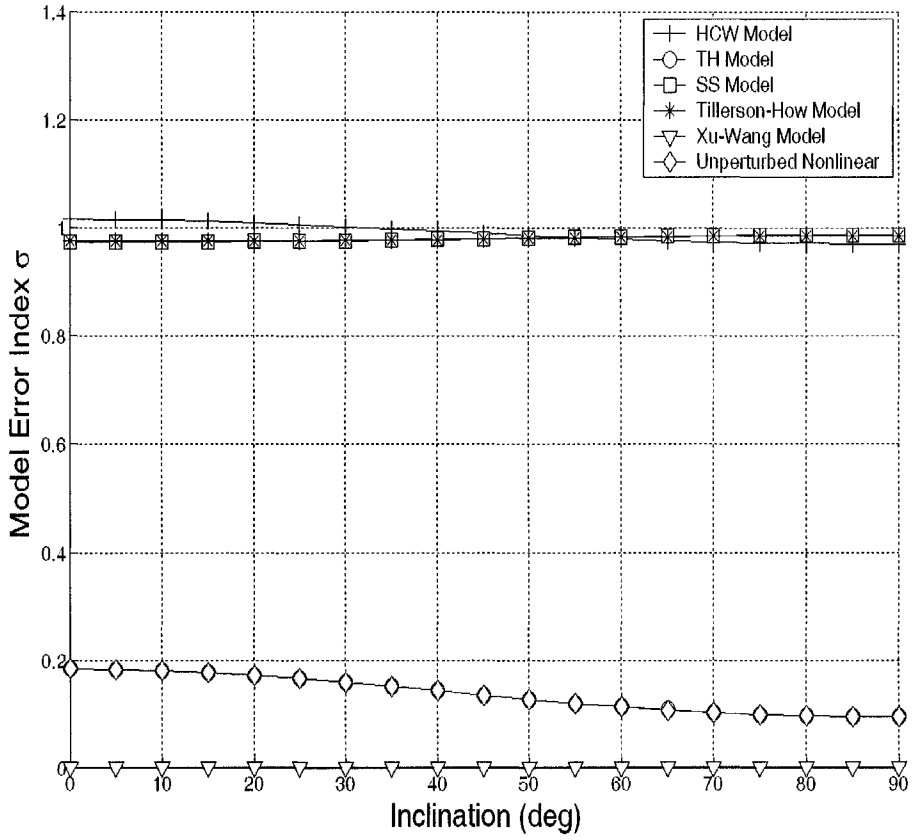

Figure 6.10: Index Comparison for $\rho = 0.1km$, $e = 0.01$, $a = 8000km$

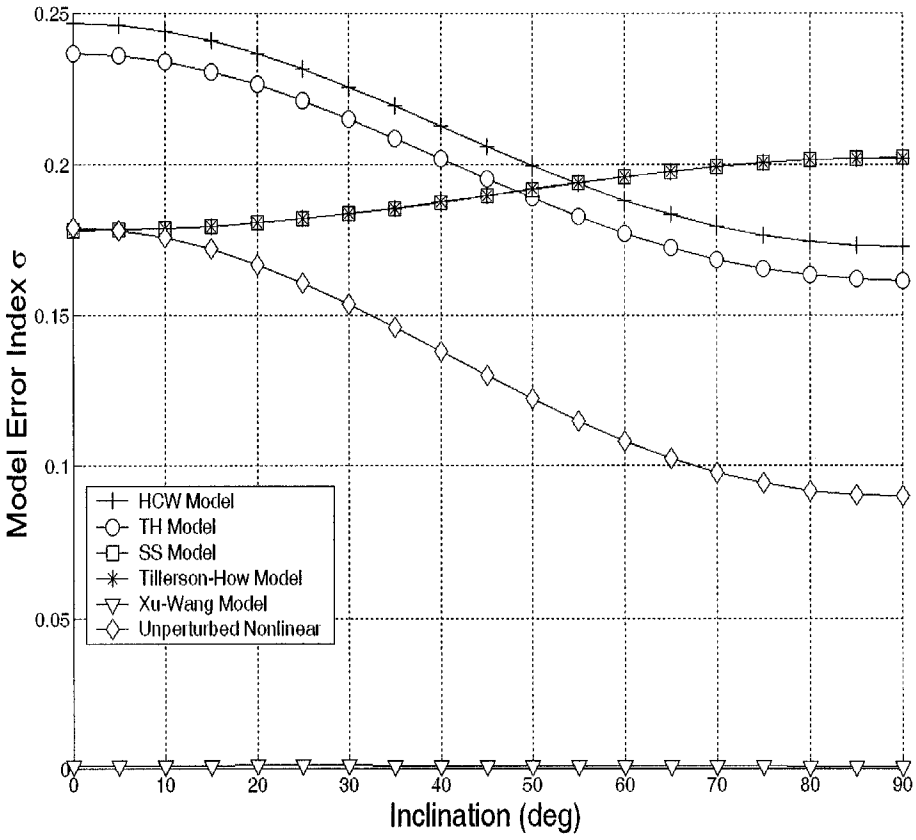

Figure 6.11: Index Comparison for $\rho = 20km$, $e = 0.0001$, $a = 8000km$

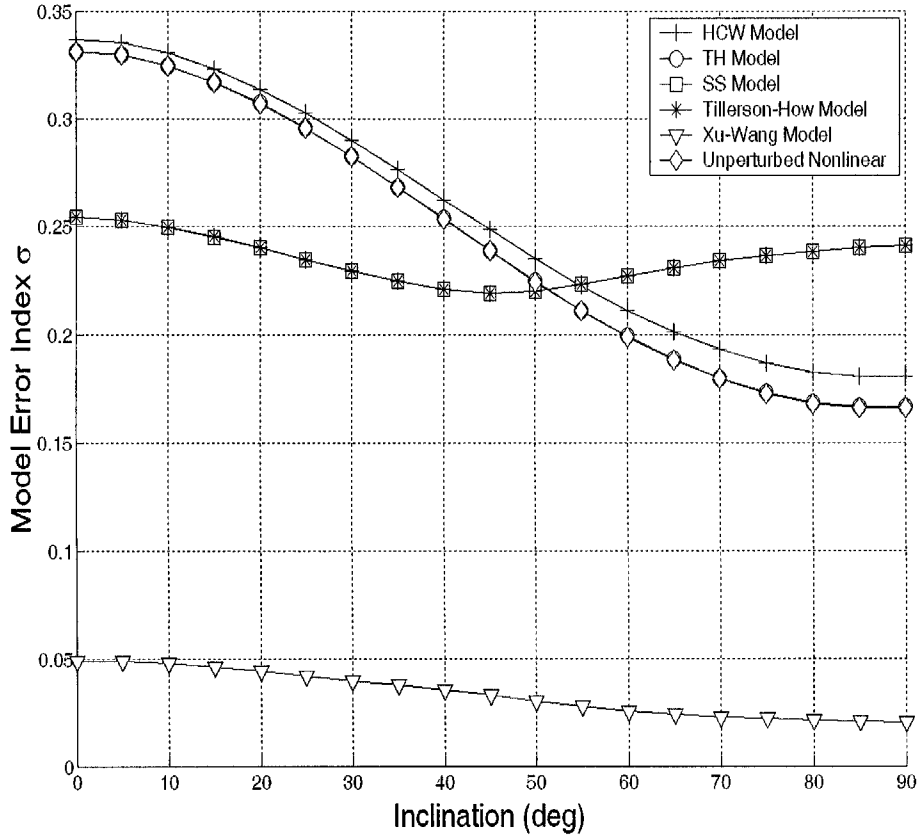

Figure 6.12: Index Comparison for $\rho = 0.1km$, $e = 0.0001$, $a = 6600km$

6.2.4 Error Index Vs Semi-major Axis a

Figure 6.13-6.14 show error index comparison as a function of chief orbit semi-major axis for various eccentricity.

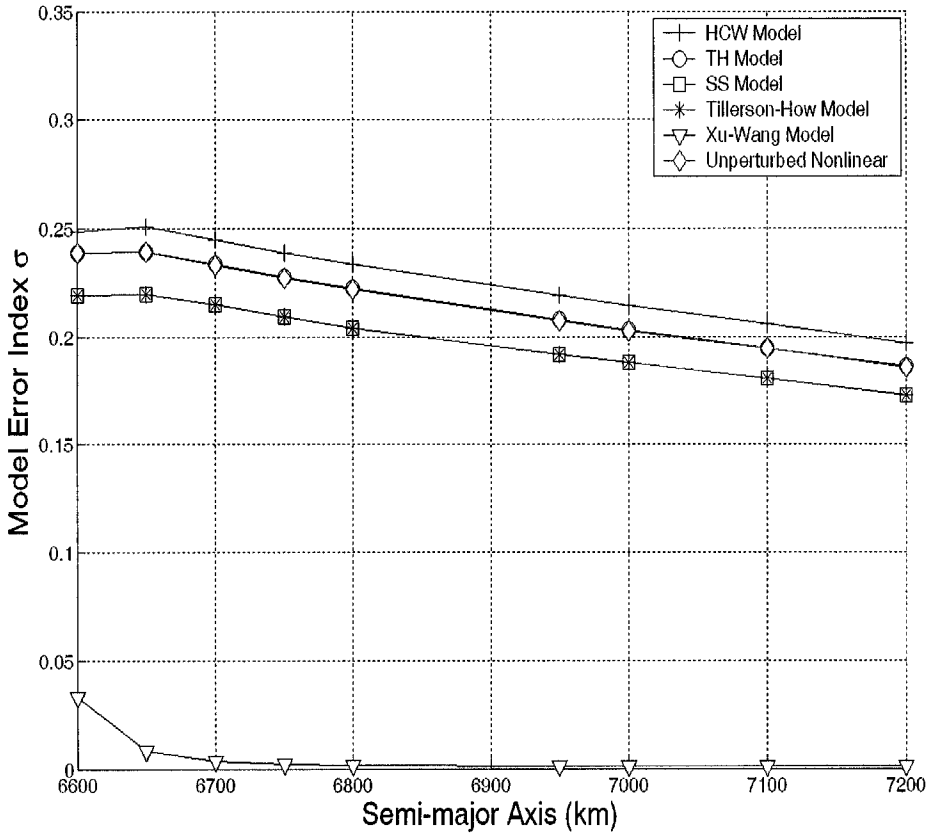

Figure 6.13: Index Comparison for $\rho = 0.1km$, $e = 0.0001$, $i = 45°$

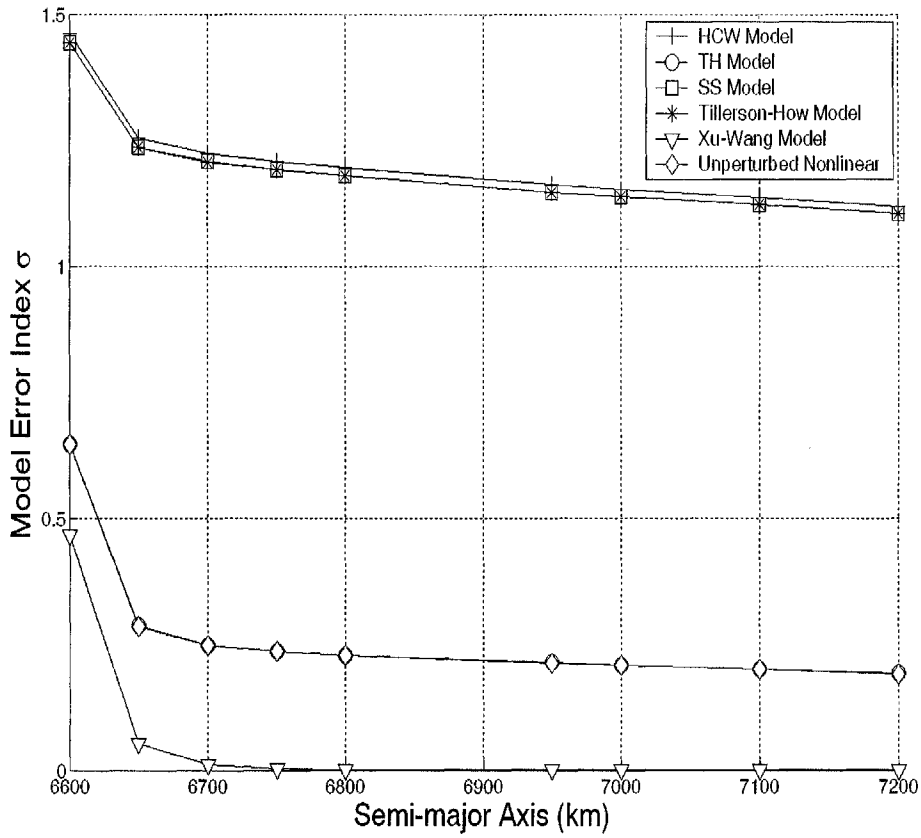

Figure 6.14: Index Comparison for $\rho = 0.1km$, $e = 0.01$, $i = 45°$

In general, Xu-Wang model performance is the best. But we can see the inflexion of all model index at semi-major axis $6800km$. That means that if chief satellite orbit semi-major axis is smaller than $6800km$, we must consider the impact of atmospheric drag. If larger than $6800km$, drag effects are relatively small.

Chapter 7

Conclusions and Future Works

7.1 Conclusions

7.1.1 Insights of Simulation Comparison

In this thesis, the effects of different orbital perturbations on dynamic models have been studied in our simulation platform. The simulation results reveal several insights into modeling satellite relative motion in space and can be summarized as follows:

- In-track initial velocity is very sensitive for formation flying. In the simulation, we found that initial condition differences between different models is $10^{-6}km/s$. A little error can lead to large drift over time. (see Section 5.2.1, Remark 5.1)
- TH model is better for compensating errors caused by elliptical chief orbit. But it does not consider J_2 effect. (see Section 5.2.2, Remark 5.2)
- Schweighart and Sedwick model is better at capturing relative motion under J_2 effect. However, it only covers case of circular chief orbit formations which

limits its application. In addition, slight drift still exists in three directions. Further improvement should be made both on modeling and initial condition derivation. (see Section 5.2.2, Remark 5.3)

- For circular chief orbit without perturbations, HCW model is an ideal model for designing satellite formations and predicting future deputy satellites relative motion. However, in practical space environment, we cannot ignore orbital disturbances, which makes error of HCW model accumulates over time and unsuitable for describing long-term formation. (see Section 5.2.3 Remark 5.4)

- Simulation results show the reference orbit eccentricity dominate the differential disturbances. And the next crucial factor on designing a stable formation is J_2 perturbation. The third one is atmospheric drag for low Earth orbit formation design. In contrast to above three factors, the effects of solar radiation pressure is small and can be ignored. (see Section 5.2.3, Remark 5.5)

A simulation-based evaluation method is presented to compare various satellite formation flying dynamic models. With the formulation of a model error index, six existing direct ODE dynamic models have been evaluated and compared in our simulation platform. The simulation results provide insights and guideline for dynamic models selection and disturbances consideration. They can be concluded as follows:

- The numerical results show that nonlinearity (formation size), chief orbit eccentricity, semi-major axis and inclination all play important roles on formation dynamic model selection. Our decision should be made through careful consideration of all four factors.

- Among all six dynamic models evaluated in our simulation, the latest Xu-Wang model performs stable and relatively best under various case scenarios.

This nonlinear model takes account of both J_2 and elliptical chief orbit disturbances, which was shown to be the two most dominant disturbances.

- As formation size become large to around $10km$, in our simulation, all linearized models errors escalated. We recommend to use nonlinear model for such application. (see section 6.2.1)

- Index comparison shows that TH model performance approaches unperturbed nonlinear model when chief orbit is highly eccentric and formation size is small. For such design cases, both models can be implemented. (see section 6.2.2)

- Schweighart and Sedwick model and Tillerson-How model have similar model errors and can perform relatively well under condition of small inclination, small formation size, and small chief orbit eccentricity. These strict conditions limits practical application of Schweighart and Sedwick model. (see section 6.2.3)

- The numerical results also show that inclination results in differential J_2 effects. Thus dynamic modeling should include inclination consideration. (see section 6.2.3)

- Atmospheric drag effects are related to satellite semi-major axis. We have to consider it if semi-major axis is less than $6800km$. Otherwise all dynamic models excluding drag consideration will lead to large model error. (see section 6.2.4)

7.1.2 Comparison of Direct ODE models

After our simulation comparison of six direct ODE models, we can conclude the situation under which the respective model is most suitable as follows: table:

Models		HCW	TH	SS	T-H	NU	X-W
Assumption	chief orbit	circle	ellipse	circle	circle	ellipse	ellipse
	perturbation	No	No	J_2	J_2	No	J_2
	formation size	small	small	small	small	large	large
Model Error caused by	eccentricity	large	small	large	large	small	nearly zero
	J_2 perturbation	large	large	small	small	large	very small
	nonlinearity	large	large	large	large	small	nearly zero

Table 7.1: Comparison of direct ODE models

Note: SS refers to Schweighart and Sedwick model. T-H refers to Tillerson-How model. NU refers to Nonlinear unperturbed model. And X-W refers to Xu-Wang model.

All the dynamic models discussed in Table 7.1 do not include atmospheric drag consideration, when chief satellite orbit semi-major axis is smaller than $6800km$, all the model errors associated are large.

7.2 Future Works

- The simulation results show that Xu-Wang model perform most stably and best under various circumstances compared with other direct ODE models. However, slight drift exists when we apply its energy matching conditions. They are crucial for formation design and fuel consumption optimization. In the near future, it will be necessary to derive the initial conditions under J_2 perturbation and obtain specific formation design based on the initial

conditions.

- For the simulation based comparison method and our model error index, they also can be used to compare other dynamic models such as models based on orbital elements differences and STM (State Transform Matrix). In future, we hope more models can be incorporated to provide detailed guideline for formation flying missions.

- Besides chief orbit eccentricity and J_2 perturbations, the atmospheric drag is an important disturbance for low Earth formation as well. In future, we hope we can find a way to include this effect into our modeling research. Future formation flying dynamic model should consider all three factors: chief satellite orbit eccentricity, J_2 perturbation and atmospheric drag effects.

Bibliography

[1] Freeflyer. *www.ai-solutions.com*.

[2] Quicksat. *users2.ev1.net/ mmccants/*.

[3] Satellite tool kit. *www.stk.com*.

[4] Satellite tracker. *www.heavenscape.com*.

[5] K.T. Alfriend and H. Yan. Evaluation and comparison of relative motion theories. *Journal of Guidance, Control and Dynamics*, 28(2):254–261, 2005.

[6] F.H. Bauer, J. Bristow, D. Folta, K. Hartman, D Quinn, and J.P. How. Satellite formation flying using an innovative autonomous control system(autocon) environment. *AIAA Guidance, Navigation, and Control Conference*, May 1997.

[7] L. Breger and J. How. Gve-based dynamics and control for formation flying spacecraft. *second International Symposium on Formation Flying Missions and Technologies*, 2004.

[8] W.H. Clohessy and R.S. Wiltshire. Terminal guidance system for satellite rendezvous. *Journal of the Aerospace Science*, pages 653–658, 1960.

[9] S. Curtis. The magnetospheric multiscale mission resolving fundamental processes in space plasmas. *NASA/TM2000-209883*, December 1999.

[10] C.P. Escoubet, R. Schmidt, and M.L. Goldstein. Cluster-science and mission overview. *Space Science Reviews*, 79:11–13, 1997.

[11] D.W. Gim and K.T. Alfriend. Satellite relative motion using differential equinoctial elements. *Celestial Mechanics and Dynamical Astronomy*, 92(4):295–336, August 2005.

[12] Pini Gurfil. Relative motion between elliptic orbits: Generalized boundedness conditions and optimal formationkeeping. *Journal of Guidance, Control and Dynamics*, 28(4), 2005.

[13] G.W. Hill. Researches in the lunar theory. *American Journal of Mathematics*, pages 5–26, 1878.

[14] J.P. How, R. Twiggs, D. Weidow, K. Hartman, and F. Bauer. Orion: A low-cost demonstration of foramtion flying in spac using gps. *AIAA*, (98-4398):48–51, 1998.

[15] G. Inalhan and J.P. How. Relative dynamics & control of spacecraft formations in eccentric orbits. *AIAA*, 2000.

[16] J.L. Junkins, M.R. Akella, and K.T. Alfriend. Non-gaussian error propagation in orbital mechanics. *Journal of the Astronautical Science*, 44:541–563, Oct-Dec 1996.

[17] N. Kasdin, P. Gurfil, and E. Kolemen. Canonical modelling of elative spacecraft motion via epicyclic obital elements. *Celestial Mechanics and Dynamical Astronomy, Springer*, 92(4):337–370, 2005.

[18] K.ed.Mortimer. Nasa-st5. *www.nasa.gov/missionpages/st5/main*, June 2006.

[19] Kong.E. and D Miller. Minimum energy trajectories for techsat 21 earth orbiting clusters. *AIAA Space Conference and Exposition 2001*, (4769), August 2001.

[20] D.J. Lee, J.E. Cochran, and J.H. Jo. Solutions to the variational equations for relative motion of satellites. *Journal of Guidance, Control and Dynamics*, 30(3):669–678, 2007.

[21] J. Leitner. Formation flying-the future of remote sensing from space. 2000.

[22] R.G. Melton. Time-explicit representation of relative motion between elliptical orbits. *Journal of Guidance, Control and Dynamics*, 23(4), July-August 2000.

[23] P.L. Palmer and E. Imre. Relative motion between satellite on neighbouring keplerian orbits. *Journal of Guidance, Control and Dynamics*, 30(2):521–528, 2007.

[24] J.P. Pluym and C.J. Damaren. Second order relative motion model for spacecraft under j_2 perturbations. *Astrodynamics Specialist Conference and Exhibit, Keystone, Colorado*, August 2006.

[25] I.M. Ross. Linearized dynamic equations for spacecraft subject to j_2 perturbations. *Journal of Guidance, Control and Dynamics*, 26(4):657–659, 2003.

[26] C. Sabol, R. Burns, and C.A. McLaughlin. Satellite formation flying design and evolution. *AAS*, page 121, 2001.

[27] H. Schaub. Spacecraft relative orbit description through orbit element differneces. *14th U.S. National Congress of Theoretical and Applied Mechanics, Blacksburg, Virginia*, June 2002.

[28] H. Schaub. Relative orbit geometry through classical orbit element differences. *AIAA Journal of Guidance, Control and Dynamics*, 27(7), September 2004.

[29] H. Schaub and K. Alfriend. J2 invariant relative orbits for spacecraft formations. *NASA GSFC Flight Mechanics and Estimation Conference*, 1999.

[30] S.A. Schweighart and R.J. Sedwick. High-fidelity linearized j_2 model for satellite formation flight. *Journal of Guidance, Control and Dynamics*, 2002.

[31] S.A. Schweighart and R.J. Sedwick. Cross-track motion of satellite formation in the presence of j_2 disturbances. *Journal of Guidance, Control and Dynamics*, 28(4), 2005.

[32] P. Sengupta, S.R. Vadali, and K.T. Alfriend. Second order state transition matrix for relative motion near perturbed elliptical orbits. *Int.J. of Celestial Mch Dyn Astr*, 97:101–129, 2007.

[33] B.D. Tapley, S. Bettadpur, M. Watkins, and C. Reigber. The gravity recovery and climate experiment: Mission overview and early results. *Geophysical Research Letters*, 31(LO9607), 2004.

[34] M. Tillerson and J.P. How. Advanced guidance algorithm for spacecraft formation-keeping. *Proceedings of American Control Conference*, 4:2830–2835, 2002.

[35] J. Tschauner and P. Hempel. Rendezvous zu einemin elliptischer bahn umlaufenden ziel. *Acta Astronautica*, 11(2):104–109, 1965.

[36] S. Vadali, S. Vaddi, K. Nai, and K. Alfriend. Control of satellite formation. *AIAA Guidance, Navigation and Control Conference*, August 2001.

[37] S.R. Vadali. An analytical solution for relative motion of satellite. *DCSSS*, 2002.

[38] D.A. Vallado. *Fundamentals of Astrodynamics and Applications.* The McGraw–Hill Companies,Inc., New York, 1997.

[39] B. Wu, V. Chu, P. Chen, and T. Ting. Formosat-3/cosmic science mission update. *GPS Solution*, 9:111–121, June 2005.

[40] G.Y. Xu and D.W. Wang. Nonlinear dynamic equations of satellite relative motion in arbitrary eccentric orbits around an oblate earth. *Accepted by AIAA Journal of Guidance, Control and Dynamics*, 2007.

[41] H. Yeh and A Sparks. Geometry and control of satellite formations. 2000.